TECHNICAL MEMORANDUM

X-395

A HOMING MISSILE CONTROL SYSTEM TO REDUCE THE EFFECTS OF RADOME DIFFRACTION

By Gerald L. Smith

Ames Research Center
Moffett Field, Calif.

NATIONAL AERONAUTICS AND SPACE ADMINISTRATION
WASHINGTON

October 1960
Declassified September 1, 1961

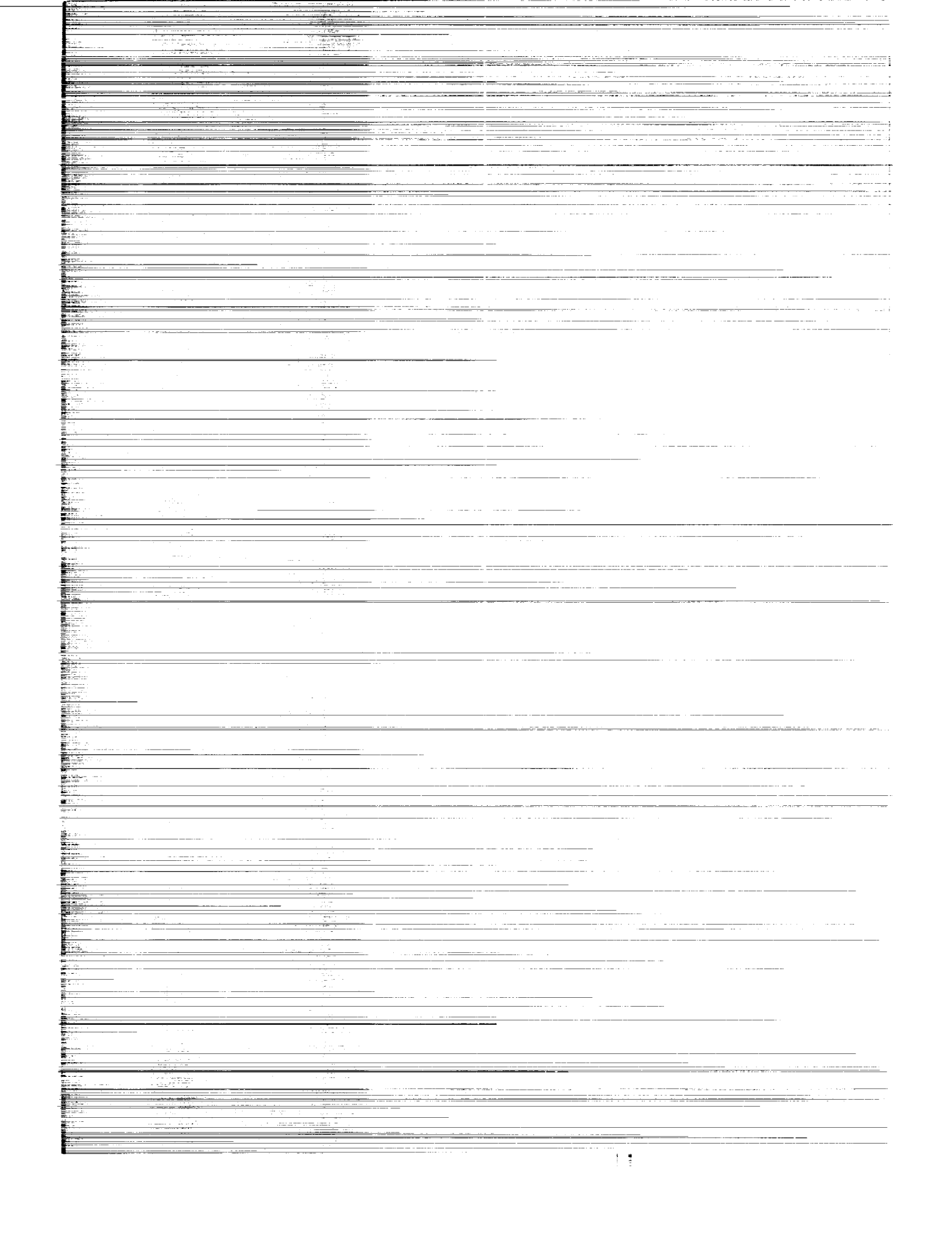

NATIONAL AERONAUTICS AND SPACE ADMINISTRATION

TECHNICAL MEMORANDUM X-395

A HOMING MISSILE CONTROL SYSTEM TO REDUCE THE EFFECTS OF RADOME DIFFRACTION

By Gerald L. Smith

SUMMARY

The problem of radome diffraction in radar-controlled homing missiles at high speeds and high altitudes is considered from the point of view of developing a control system configuration which will alleviate the deleterious effects of the diffraction.

It is shown that radome diffraction is in essence a kinematic feedback of body angular velocities which causes the radar to sense large apparent line-of-sight angular velocities. The normal control system cannot distinguish between the erroneous and actual line-of-sight rates, and entirely wrong maneuvers are produced which result in large miss distances.

The problem is resolved by adding to the control system a special-purpose computer which utilizes measured body angular velocity to extract from the radar output true line-of-sight information for use in steering the missile. The computer operates on the principle of sampling and storing the radar output at instants when the body angular velocity is low and using this stored information for maneuvering commands. In addition, when the angular velocity is not low the computer determines a radome diffraction compensation which is subtracted from the radar output to reduce the error in the sampled information.

Analog simulation results for the proposed control system operating in a coplanar (vertical plane) attack indicate a potential decrease in miss distance to an order of magnitude below that for a conventional system. Effects of glint noise, random target maneuvers, initial heading errors, and missile maneuverability are considered in the investigation.

INTRODUCTION

Diffraction of electromagnetic radiation by the radome which encloses the radar antenna is known to result in a serious deterioration in the performance of homing missiles under certain conditions. These conditions exist, for instance, when a cruciform tail-controlled missile is employed in high-speed, high altitude attacks. The trouble arises because such a missile, in order to maneuver rapidly, must experience rather large body angular velocities so that the required high angles of attack may be developed quickly. In so doing, the look angle (angle at which radiation reflected from the target enters the radome) changes rapidly. Since the radome diffraction changes with look angle, an apparent change of the line-of-sight angle is generated whenever the missile maneuvers. Even with the modest amounts of radome diffraction present in good radomes, these apparent line-of-sight changes can be as much as an order of magnitude greater than any real change in the line-of-sight angle which could ever be expected. The normal control system cannot distinguish between the erroneous and actual line-of-sight information and it is apparent that entirely wrong maneuvers are certain to result.

Radome diffraction can be considered from a slightly different point of view as an unwanted element of the missile control system, namely coupling of body angular velocity into the radar tracking system. In control system terminology this is a feedback which if sufficiently great (as it is at high altitudes with a reasonably fast autopilot) renders the control system unstable and therefore incapable of performing its intended function. The usual means employed to assure stability in this situation is simply to reduce the system loop gain. This can be done by reducing the autopilot gain, that is, by making the autopilot sluggish. However, degradation of autopilot performance means that the system will not be able to respond rapidly to line-of-sight information and quite large miss distances are likely to be experienced except in the least demanding of attack situations.

It is apparent that some means is desired of reducing radome diffraction feedback which will not result in a severe sacrifice in performance. This objective could be achieved by the development of superior radomes, by elimination of the radome altogether, or by changing the missile configuration to one which does not require large angles of attack. Such methods are under wide investigation (e.g., refs. 1 and 2) but invariably involve important problems in regard to practicability. A possible simpler alternative is to accept existing radome and missile configurations and seek a solution within the control system itself. This is the approach followed here. The basic principle exploited is that there exists within the control system unused information which if properly utilized can effect a marked reduction in radome diffraction feedback while maintaining efficient normal system operation. Utilization

TABLE OF CONTENTS

of this additional information is realized by adding to the control system a special-purpose computer of simple design.

The task undertaken in this study involves the synthesis of an efficient control system. Unfortunately the system involved is of a complex nonlinear and time-varying nature for which analytical methods are not readily applicable. This necessitates recourse to a trial and error approach described in the following sections of the paper. First, a hypothetical system configuration is developed by the logical application of basic principles. Then an effort is made to establish design criteria by means of a discussion of the influence of the system inputs and inherent restrictions in the problem. Finally, the results of a simulation study are presented, in terms of the design of a specific system and an evaluation of the system's performance.

NOTATION

A	gate level, volts (normalized to 1 volt per radian/sec)
a_c	autopilot command, volts (normalized to 1 volt per ft/sec^2)
a_M	missile normal acceleration, ft/sec^2
e	error between missile and target position, $y_T - y_M$, ft
G_C	open-loop pseudo transfer function of k-compensation system
k	radome error slope, $\frac{\partial \epsilon}{\partial \beta}$, radian/radian
k'	computed radome error slope, radian/radian
Δk	error in k-computation, k-k', radian/radian
K_a	autopilot gain
K_A, K_{B1}, K_{B2}	autopilot rate feedback gains
K_{C1}, K_{C2}	k-compensation system gains
K_H	sample-and-hold-circuit open-loop gain
s	Laplace transform variable
v	voltage output of the radar system
v_1, v_2, v_3	computer internal voltages

V_M	missile velocity, ft/sec
V_R	closing velocity, ft/sec
V_T	target velocity, ft/sec
y_M	missile displacement perpendicular to the reference line of sight, ft
y_N	apparent target displacement due to glint noise perpendicular to reference line of sight, ft
y_T	target displacement perpendicular to reference line of sight, ft
Y_R	transfer function of the radar system
α	angle of attack, radians
β	look angle, radians
β_o	initial look angle, radians
$\dot{\gamma}$	rate of change of the flight path angle, radians/sec
δ	control surface deflection, radians
ϵ	radome diffraction angle, radians
$\dot{\theta}$	pitch rate, radians/sec
$\dot{\theta}_R$	pitch rate modified by radar dynamics, volts (normalized to 1 volt per radian/sec)
λ	control system gain
λ_o	initial value of control system gain
σ	line-of-sight angle with respect to horizontal reference, radians
σ_a	apparent line-of-sight angle with respect to horizontal reference, $\sigma-\epsilon$, radians
$\dot{\sigma}_R$	line-of-sight rate modified by radar dynamics, volts (normalized to 1 volt per radian/sec)
τ	time remaining until intercept, sec

ψ_o initial angle between line-of-sight and ideal missile flight path

$(\dot{}),(\ddot{})$ first and second time derivatives of ( )

THEORY OF THE MODIFIED CONTROL SYSTEM

Assumptions

A homing missile control system of conventional configuration is assumed as a point of departure in the analysis which follows. Such a system consists principally of (1) a tracking radar with a servo-controlled rotatable antenna, and (2) an autopilot which stabilizes the missile and controls its maneuvers in accordance with commands supplied to it from the radar. A tail-controlled missile of symmetrical configuration about the longitudinal axis is assumed. Thus, the control system has two more or less identical channels, one for the elevation or pitch axis, and one for the azimuth or yaw axis. The autopilot also provides roll stabilization, a function which is assumed to be independent of the pitch and yaw channels of the control system. For simplicity only the pitch channel is considered here, and it is assumed that negligible cross coupling exists between channels.

The Computer

In the INTRODUCTION the potential instability introduced by radome diffraction has been briefly described, and it has been stated that a control system modification is sought which will eliminate the difficulty arising from this phenomenon. To provide a feeling for the sort of modification that might be appropriate, a detailed analysis of the situation will now be developed, employing a time domain approach for clarity.

The nature of the radome diffraction phenomenon is described in the appendix, where the geometry involved is given (fig. 13) and the equations are developed which are required here. It is shown that radome diffraction can be regarded as the feedback of body angular velocity into the control system input. In reference to the pitch channel of the control system, this is a feedback of pitch rate, $\dot{\theta}$, as illustrated in sketch (a). Here the input to the control system is $\dot{\sigma}$ (the line-of-sight angular velocity) and the output is a_M (the acceleration developed by the missile). Added to the input $\dot{\sigma}$ is a perturbation $k\dot{\theta}$ generated by radome diffraction when the missile maneuvers. It is to be noted that the diffraction feedback parameter k is a function of the look angle β (not shown explicitly in

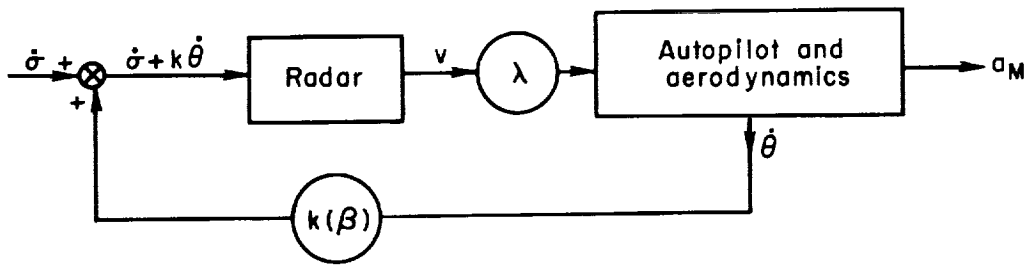

Sketch (a)

sketch (a)), so that the feedback is nonlinear. The entire gain of the control system is shown lumped into the single gain parameter, λ, for convenience in the discussion.

In sketch (a) it is seen that the radar input is $\dot{\sigma} + k\dot{\theta}$, where the dimensions are in radians per second. For convenience, the radar gain is normalized so that its steady-state output is 1 volt for a 1 radian per second input. The output voltage, v, then may be represented as

$$v = \dot{\sigma}_R + (k\dot{\theta})_R \tag{1}$$

where the R subscript is employed to denote modification produced by the radar dynamics. The term $\dot{\sigma}_R$ represents the line-of-sight information which is required for steering the missile, whereas the term $(k\dot{\theta})_R$ represents erroneous information generated during maneuvers because of the radome error slope, k.

Some idea of the magnitudes of the various quantities appearing in equation (1) is desirable to lend credence to the arguments that follow. The maximum magnitude of the line-of-sight rate, $\dot{\sigma}$, generally occurring at the time of launch, can be expected to be on the order of 0.0025 radian/sec for a good homing system. A good radome may have a maximum error slope, k, of something like 0.05 radian/radian, and a missile of the type considered here should be capable of developing maximum pitching rates of about 0.5 radian/sec if it is to maneuver reasonably fast. It is seen then that the magnitude of the $(k\dot{\theta})_R$ term in equation (1) could easily be on the order of 10 times as great as the $\dot{\sigma}_R$ term, and instability could surely result if nothing were done about the situation.

Now consider a hypothetical time history of v as shown in sketch (b). Here, a positive constant k is assumed for simplicity, and a missile maneuver begins at $t = a$. During the time the missile is building up an angle of attack, a large perturbation due to $(k\dot{\theta})_R$ is generated, whereas the true value of $\dot{\sigma}_R$, represented by the dotted curve, changes very little (by the very nature of the line-of-sight rate). After the transient has subsided at $t = b$, v again becomes a good representation of $\dot{\sigma}_R$. This analysis suggests that in the interval $a < t < b$, it would be best to disregard any changes in v so far as using this quantity to command the autopilot is concerned and to use instead the value of v at $t = a$. Such a procedure would amount to inserting between the radar and autopilot a sample-and-hold circuit which gates the radar voltage through as an autopilot command only when the

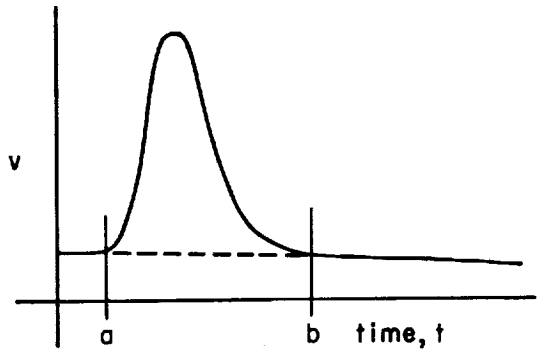

Sketch (b)

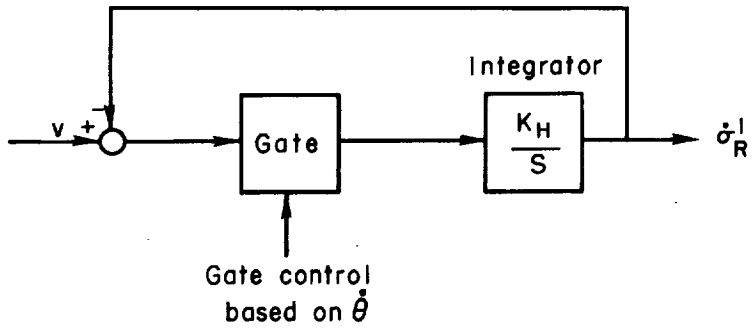

Sketch (c)

radome diffraction perturbation in v is small, and holds the latest reliable value of v when the perturbation is large. The output of the sample-and-hold circuit (sketch (c)) is then a measure of $\dot{\sigma}_R$ which may be designated $\dot{\sigma}_R'$ to denote that it is not exactly equal to $\dot{\sigma}_R$.

Now consideration must be given to the feasibility of instrumenting the desired gating control, which depends upon determining when the perturbation $(k\dot{\theta})_R$ is zero (or very small). To see how this might be

done, consider first the quantity $k\dot{\theta}$, which it is seen can be zero when either k or $\dot{\theta}$ is zero. Then it is noted that this quantity, $k\dot{\theta}$, is zero at somewhat different times than $(k\dot{\theta})_R$ because of the radar time lags, the closeness of occurrences of $(k\dot{\theta})_R$ zeros and $k\dot{\theta}$ zeros depending for the most part on the speed of the radar. Thus, faced with the problem of determining the zeros of $(k\dot{\theta})_R$, it is seen that those due to the changing k cannot be detected at all since k is unknown, but that the remaining zeros can be detected (at least approximately) by considering their relationship to the zeros of $\dot{\theta}$. Intuitively, it appears that if $\dot{\theta}$ (as measured by a rate gyro) were subjected to the same dynamic modification as is imposed upon $k\dot{\theta}$ by the radar, the zeros of the resultant quantity, $\dot{\theta}_R$, would coincide fairly closely with the detectable zeros of $(k\dot{\theta})_R$, and this is the approach taken here. It should be possible, then, to achieve reasonable gating accuracy by having the gate close whenever the magnitude of $\dot{\theta}_R$ is very small.

There is a complication, however, which arises from the operational interaction of the hold circuit and the autopilot. It should be realized that during a $\dot{\theta}$ transient (i.e., $|\dot{\theta}_R|$ large), the output of the hold circuit will remain constant, thus applying a constant acceleration command to the autopilot. When this command is not zero, it is seen that $\dot{\theta}_R$ does not return to zero after its transient but rather to the constant value of $\dot{\gamma}$ associated with the a_M developed. If the gate level is smaller than this value of $\dot{\gamma}$, the gate will not reopen. One way to avoid this difficulty would be to employ a gate level larger than the maximum $\dot{\gamma}$ which can be developed by the missile, but this is awkward in that the maximum $\dot{\gamma}$ is a function of altitude. An alternative which is employed here because it appears more practical is to use as a gating signal the quantity $\dot{\alpha}_R = (\dot{\theta} - \dot{\gamma})_R$, whose steady-state value is zero.[1] Thus, the gate control is designed so that the gate is closed when $(\dot{\theta} - \dot{\gamma})_R$ is smaller than a chosen gate level, A (or, equivalently, when $(\dot{\theta} - \dot{\gamma})_R^2$ is smaller than A^2). Then the gate level theoretically may be made as arbitrarily small as desired.

Even with $A = 0$ it is seen from the foregoing discussion that the gating cannot be perfect since the gating signal is not perfect, with the result that some residual radome diffraction error must always appear in $\dot{\sigma}_R'$. Assuming the response time of the sample-and-hold circuit to be

[1]It should be noted that for the type of missile considered, the $\dot{\theta}$ contribution to the $\dot{\alpha}$ transient is overwhelmingly larger than $\dot{\gamma}$ at high altitudes, so the approximation $\dot{\alpha} \approx \dot{\theta}$ is reasonable during the transient period. Instrumentation of $\dot{\alpha}$ as a gating signal is most easily done in the form $\dot{\alpha} = \dot{\theta} - (a_M/V_M)$, where $\dot{\theta}$ and a_M are measured by a rate gyro and an accelerometer, respectively, and V_M can be assumed constant. The magnitude of $\dot{\alpha}_R$, or equivalently $\dot{\alpha}_R^2$, is required for gating, $\dot{\alpha}_R^2$ being employed here for convenience.

suitably small, the output $\dot{\sigma}_R'$ during a gate-open period can be written as

$$\dot{\sigma}_R'(t) = \left[\dot{\sigma}_R\right]_a + \left[(k\dot{\theta})_R\right]_a \qquad \text{for } a < t < b \tag{2}$$

where the subscript a refers to the instant of time when the gate opens, and b is the time the gate closes. The residual error in $\dot{\sigma}_R'$ is represented by the term $\left[(k\dot{\theta})_R\right]_a$.

Since the sample-and-hold system cannot remove all the radome diffraction perturbation from the autopilot command, it is appropriate to consider the possibility of obtaining better performance by a further utilization of the radar and $\dot{\theta}$ information. Refer to sketch (b) again and consider the fact that during the period $a < t < b$, the change in v, $v(t) - v(a)$, which is discarded as far as autopilot command information is concerned, represents a fair measure of the $(k\dot{\theta})_R$ term in v. This then might be the basis for an in-flight computation of k which could be utilized in a compensation scheme to reduce the effective magnitude of the unwanted radome diffraction feedback. The idea is to compute from the radar output during periods of large perturbation a measure of k which is as up-to-date as possible. This measure of k, which might be called k' to denote the fact that it is not exactly equal to k, can be stored in the computer to provide a compensating voltage, $(k'\dot{\theta})_R$, to be subtracted from the radar voltage. The compensated radar voltage then would be

$$v_1 = v - (k'\dot{\theta})_R = \dot{\sigma}_R + (\Delta k\dot{\theta})_R \tag{3}$$

where $\Delta k = k - k_1$. If v_1 is then used as the input to the sample-and-hold circuit instead of v, the output will be

$$\dot{\sigma}_R'(t) = \left[\dot{\sigma}_R\right]_a + \left[(\Delta k\dot{\theta})_R\right]_a, \qquad a < t < b \tag{4}$$

The residual perturbation which gets through to the autopilot is then $\left[(\Delta k\dot{\theta})_R\right]_a$. This should be materially smaller than would exist if compensation were not employed since it is hoped that Δk on the average would be substantially smaller in magnitude than k.

A circuit for computing the k-compensation is shown in sketch (d). To begin with it is assumed that a reasonably accurate measure of the

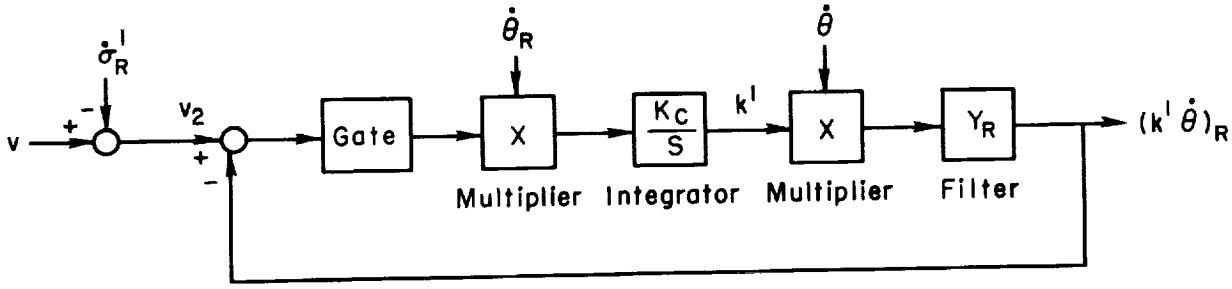

Sketch (d)

true line-of-sight rate, $\dot{\sigma}_R'$, is available from the output of the sample-and-hold circuit. When this is subtracted from v, the remainder is

$$v_2 = (\dot{\sigma}_R - \dot{\sigma}_R') + (k\dot{\theta})_R \tag{5}$$

If the difference quantity $(\dot{\sigma}_R - \dot{\sigma}_R')$ is assumed to be small, v_2 is given approximately by

$$v_2 \approx (k\dot{\theta})_R \tag{6}$$

the validity of the approximation being dependent on the magnitude of $(k\dot{\theta})_R$. The voltage v_2 is then applied to the input of a closed-loop servo system, the output of which follows v_2 to produce a quantity defined as the compensating voltage, $(k'\dot{\theta})_R$. A gate which operates in a sense opposite to that of the sample-and-hold circuit gate is employed in the forward loop to prevent interaction with the sample-and-hold circuit. That is, the gate closes when $|\dot{\theta}_R - \dot{\gamma}_R| > A$, or during periods of large radome diffraction perturbation, and computation takes place only during such periods. It is seen that because of the $\dot{\theta}$ multiplier and Y_R filter following the integrator in the forward loop, the integrator output is k'.

The multiplication by $\dot{\theta}_R$ preceding the integrator is employed so that the polarity of the loop gain will not depend on the polarity of $\dot{\theta}$. In addition, this multiplier (together with the $\dot{\theta}$ multiplier following the integrator) serves the purpose of making the loop dynamics a function of $\dot{\theta}_R$, so that the system response is sluggish when $\dot{\theta}_R^2$ is small and becomes more rapid as $\dot{\theta}_R^2$ increases. The reason for this is that the $\dot{\sigma}_R - \dot{\sigma}_R'$ component of v_2 tends to cause k' to be in error by the amount $(\dot{\sigma}_R - \dot{\sigma}_R')/\dot{\theta}_R$ if the system is sufficiently fast. Such an error could

be intolerable at the beginning and end of the computation period when $|\dot{\theta}_R|$ is small. This difficulty is avoided if the loop dynamics are such that when $|\dot{\theta}_R|$ is small the system does not follow well and thus tends to ignore the error-producing quantity. Of course, the system then does not follow changes in k very well either when $|\dot{\theta}_R|$ is small, but it is noted that k is not changing very fast when $|\dot{\theta}_R|$ is small anyway and therefore little error should ensue from this. The intended result is for the system to maintain k' as a reasonably good up-to-date measure of k. When the gate opens at the end of a computation cycle, the loop is broken, and the integrator holds the last computed value of k' to provide compensation during the sampling interval which follows.

When the sample-and-hold and k-compensation circuits are combined, the result is a computer whose relation to the remainder of the control system is shown in simplified form in figure 1. For convenience, it is assumed that the autopilot and instrument gains are normalized so that a 1 volt input to the autopilot is a 1 ft/sec^2 acceleration command, and the output of the pitch rate gyro is 1 volt per radian/sec. The computer inputs are then $\dot{\theta}$ and v, and its output is employed as an acceleration command, a_c, when the autopilot activation switch is closed. The system gain, λ, is assumed to be contained in the computer for convenience in later discussion.

The complete computer is shown in block diagram form in figure 2. It will be noted that in the course of combining circuits, some minor changes have been introduced which do not alter the basic mode of operation. First, since the gate control is the same for both circuits, the two gates are combined to operate as a double-throw switch, connecting v_3 to the hold circuit integrator when $|\dot{\theta}_R - \dot{\gamma}_R|$ is small and to the compensation circuit when $|\dot{\theta}_R - \dot{\gamma}_R|$ is large. Second, for simplicity the quantity $(\dot{\theta} - \dot{\gamma})_R$ is used as a multiplier instead of $\dot{\theta}_R$ in the compensation circuit since an additional Y_R filter would be required to obtain $\dot{\theta}_R$.[2] Third, the system gain, λ, is inserted in two parts, a term λ/λ_o preceding the hold circuit and a term λ_o following the hold circuit. This merely alters the open-loop gain of the compensation circuit and changes the voltage level in the hold circuit. The reason for this arrangement will be explained later. Fourth, a by-pass amplifier around the integrator in the k-compensation circuit has been added to provide a lead term which is required for good dynamic performance.

The appearance of three multipliers in the computer would seem on the surface to render the proposed system too complex for use in an expendable missile. However, highly accurate multiplications are not likely to be required because the multipliers are in a closed-loop system which is inherently insensitive to internal errors. Thus, approximate multiplication

[2]An analog simulation study showed that this arrangement makes no apparent difference in the system operation.

by simple electronic devices should be adequate. Also several alternative design possibilities exist, such as employing a specially designed rate gyro directly as a multiplying device. Without going into further detail, it is sufficient to say that no more than normal design ingenuity should be necessary to achieve a simple and compact realization of the system described.

Remainder of the Control System

Integration of the proposed computer with the remainder of the control system will now be considered. A little thought will show that the operation of the sample-and-hold system and the autopilot are strongly interdependent. After the gate opens the acceleration command, a_c, applied to the autopilot remains fixed until $(\dot{\theta} - \dot{\gamma})_R$ returns to zero. In the period during which $(\dot{\theta} - \dot{\gamma})_R$ is not small the missile is developing an acceleration, a_M, in response to the command, a_c, and the length of this period will depend on the dynamics of the autopilot-aerodynamics combination. As soon as $(\dot{\theta} - \dot{\gamma})_R$ returns to zero the gate closes, a new value of a_c is applied to the autopilot and a new maneuver begins, whereupon the gate reopens. It is seen, therefore, that a_c is likely to be a staircase-type function, the steps of which have an average period determined by the autopilot-missile dynamics, and $\dot{\theta}$ will appear as a series of pulselike transients, one associated with each step change in a_c. The conclusion to be drawn from this analysis is that the autopilot must be fairly fast so that the gate will close frequently enough to make a_c a reasonably up-to-date measure of $\dot{\sigma}$.

The role of the radar system has been discussed on page 8. It is sufficient to say that the radar tracking loop should be fairly fast so as to minimize the effect the radar dynamics have upon the accuracy of gating.

The choice of the control system gain, λ, determines the over-all homing performance of the missile and must take into consideration the outer loop homing kinematics which are a function of the attack situation (i.e., the missile and target velocities and the attack aspect). Normally the value of λ is adjusted prior to launch to suit the particular attack conditions. As far as the radome diffraction problem is concerned, it is seen that increasing λ increases the sensitivity of the system to the unwanted feedback, $k\dot{\theta}$, and this increases the difficulty of eliminating trouble from this source. Therefore, the smallest value of λ which meets the requirements of satisfactory homing should be employed. However, this is not the whole story regarding λ. Up to this point the questions of noise and limits on the missile acceleration have been

purposely ignored to avoid confusion. When these factors are considered it will be seen that λ should not be constant but should vary during the flight as a function of the range.

INFLUENCE OF SYSTEM INPUTS ON THE DESIGN

So far system design criteria have been discussed solely in terms of the disturbing influence of radome diffraction. If this were the only factor, the design could be worked out entirely in terms of maximizing the line-of-sight information content of a_c while minimizing the radome diffraction error in a_c. Unfortunately, the problem is not so simple. In the first place, noise is apt to have an important disturbing influence on system performance. In the second place, the missile acceleration is severely limited (especially at high altitudes) and consideration must be given to the efficient use of the available acceleration if a small miss distance is to be achieved.

The most important type of noise in radar-controlled missile systems is that produced by target scintillation (also called glint noise). Typically, this phenomenon appears as a random apparent target displacement with a spectrum which is virtually white; that is, its band width is much wider than that of the control system. Other types of noise also will exist in any real system but their effects will not be unlike those of target scintillation and, for simplicity, only the latter is considered here explicitly.

The manner in which noise-induced disturbances are propagated through the control system is as follows. In the output of the radar, glint noise produces random apparent line-of-sight angular velocities. These fluctuations are small at launch when the target is far from the radar and increase in magnitude as the missile approaches the target. The noise gets through the computer to show up in a_c in two ways. First, the sample-and-hold circuit does not distinguish between the true signal and the additive noise, and thus will sample and then hold line-of-sight information which is in error because of the noise. Second, the noise produces errors in the computation of k' in the k-compensation system and these errors are passed on to a_c as noise-induced values of $\left[(\Delta k\dot{\theta})_R\right]_a$. The disturbances so induced in a_c are primarily at low frequencies (because of the sample-and-hold operation), and will be readily followed by the autopilot.

Consider now how the over-all performance of the system is influenced by the noise. This is best understood in terms of the limits on the missile acceleration. If the disturbances due to the noise are appreciable, rather large deviations from the ideal missile trajectory will

occur which may take the missile far enough off course that it will not be able to maneuver late in the flight to obtain a hit (or suitably small miss distance). Thus, it is mandatory that suitable precautions be taken in designing the system to insure that the disturbances in a_c are not excessive. Inevitably, attempts to reduce disturbance effects will result in an impairment of the ability of the system to respond to line-of-sight information and to discriminate against radome diffraction perturbations. The best tactic therefore involves a compromise of the sort which is implicit in most statistical optimization methods (see ref. 3). The idea is to employ noise-reduction techniques, the simplest of which is filtering, only to the point where further reduction of the noise permits other causes to produce a greater increase in miss than the decrease achieved by the noise reduction. Because of the nature of the nonlinearities involved in the present problem, analytical methods for implementing such a design procedure do not appear feasible. Nonetheless, the results of reference 3 can be used as a guide. Particularly pertinent in that study is the fact that the optimum system requires a fair percentage of its maximum acceleration to follow disturbances. Thus, it seems reasonable here to employ only enough noise discrimination to keep the rms acceleration within say 50 percent of the maximum missile acceleration. This should leave enough capability for adequate correction of launch errors and for following of target maneuvers. Such a procedure, of course, will not yield an optimum system, but at least it is a technique which can be utilized readily in the trial-and-error design approach, and, as will be seen, leads to acceptable results.

The manner in which noise discrimination may be achieved in the control system may now be discussed. As indicated previously, the autopilot itself cannot perform any significant filtering because the disturbances in a_c have nearly the same band width as the autopilot. Therefore, the filtering must be done in the radar and computer. Nevertheless, it can be seen that the autopilot design has an indirect effect on noise discrimination because a fast autopilot develops high pitch rates and therefore large radome diffraction perturbations which the computer will have more difficulty removing. An autopilot that is only modestly fast then can relax the requirements in the computer so that it can perform some noise filtering. Such filtering can be obtained by increasing the gate level and the sampling circuit time constant slightly from their ideally zero values. Similarly, the k-compensation loop gain can be reduced so that the system does not follow the noise too readily but still is fast enough to keep Δk reasonably small. The radar time constants can likewise be increased to reduce the noise level in the radar output but again not so much as to produce an excessive adverse effect on the accuracy of the gating operation.

The reasoning underlying the choice of the system gain, λ, remains to be explained. In reference 3 it is shown that a homing missile control system optimized for operation in the presence of glint noise has a gain

which decreases as the flight progresses, although it should be realized that true optimization involves more than simply employing a time-varying gain. The function of the time-varying gain is to prevent the increasing noise from saturating the system. Clearly the same situation exists in the present study, the only difference being that the choice of an appropriate λ function is more a matter of trial and error than it was in reference 3. Of various possible locations for this time-varying element the best seems to be within the computer, just ahead of the sample-and-hold circuit, as shown in figure 2. In this location not only is the noise magnitude attenuated directly as the noise increases but also the k-compensation loop gain (and hence its speed of response) is decreased as the noise increases, improving the ability of the k-compensation system to reject the noise.

THE ANALOG SIMULATION STUDY

To test the theory of the control system modification presented in the preceding section, an analog computer simulation study was undertaken. The objective of the study was to design, by trial and error methods, a practical system, and then to test the system in a simulated attack situation. For comparison purposes, a so-called perfectly compensated system (i.e., with no radome diffraction) and a sluggish system with radome diffraction were tested in the same attack situation. This procedure is described in the following paragraphs.

Description of the Task

To avoid unreasonable complication it was necessary to restrict the computer study to a single situation described by those factors which the control system designer is not at liberty to alter. These factors are the tactical situation (or outer loop kinematics), the system inputs, the missile aerodynamics, the intrinsic limitation on missile maneuverability, and the radome diffraction characteristic. Judicious assumptions regarding these factors insure that a realistic and fairly difficult (but not impossible) task is presented to the missile and its control system.

The tactical situation assumption is that the target airplane flies at 1500 ft/sec at an altitude of 100,000 feet and that the missile-launching interceptor is directly in the path of the target but 10,000 feet lower and 150,000 feet from the target at the instant of launch. The missile thus must climb 10,000 feet as well as follow any maneuvers undertaken by the target during the attack. A missile velocity of 4700 ft/sec, constant throughout the attack, is assumed, and the missile body and its

velocity vector are assumed to be horizontal at launch. The geometry of the situation as described is shown in figure 3, where the initial line-of-sight is indicated as MT and the initial look angle, β_o, is 0.067 radian. The ideal flight path to intercept is MI and depends upon V_T, V_M, and the geometry of the attack.

Of course, this path is not actually followed because the missile is headed wrong initially and because the target may maneuver during the attack. However, the triangle MTI provides a useful reference frame for purposes of linearizing the geometry under the assumptions that the target and missile flight paths will not depart markedly from TI and MI, respectively. The linearization is the same as that used in reference 3 and gives a constant closing velocity, V_R, of 6196 ft/sec and an attack duration of 24 seconds.

The inputs assumed for the study are threefold: (1) the initial heading error, $\beta_o + \psi_o$; (2) a target maneuver consisting of random ±1 g acceleration turns in the vertical plane, the switching occurring at the average rate of one every 5 seconds; (3) glint noise equivalent to an rms apparent target displacement of 30 feet with an essentially white spectrum. The random target maneuver is seen to be the same as that employed in reference 3 and is more fully described there. The noise is also the same as in reference 3 except for being of somewhat smaller magnitude.

Description of the Missile

Linearized aerodynamics are assumed which are representative of a typical tail-controlled missile at the assumed speed and altitude. These aerodynamics are expressed in the form of the following equations of motion:

$$\left.\begin{aligned} \dot{\alpha} &= \dot{\theta} - 0.070\,\alpha - 0.0062\,\delta \\ \ddot{\theta} &= -10.9\,\delta - 16.9\,\alpha - 0.023\,\dot{\theta} \end{aligned}\right\} \qquad (7)$$

The assumption made regarding missile maneuverability is that the controls are limited to a travel of ±0.5 radian. For the aerodynamics indicated in equations (7) and the assumed missile velocity of 4700 ft/sec, this corresponds to limits of ±2.86 g on acceleration. Since the vertical plane is considered in this study, a 1 g bias must be subtracted from these limits to account for the level flight trim condition. The true maneuverability limits are thus +1.86 g and -3.86 g.

The final assumption to be made is in regard to the radome error slope characteristic, k. Since the system operation is likely to be

critically dependent on the nature of this characteristic, a realistic representation must be employed. Such a characteristic, constructed arbitarily as being typical of curves appearing in the radome literature (for examples see refs. 1 and 2), is shown in figure 4.

The Problem Simulation

The manner in which the single-channel (coplanar attack) homing missile problem was simulated on the analog computer is shown in simplified form in figure 5. The time-varying range inherent in the homing problem is represented by a time-varying gain as shown (division by τ, time remaining until intercept). The multiplication of a_M by $\cos \psi_o$ in the outer feedback loop is required to obtain the component of a_M perpendicular to the reference direction which is the initial line of sight, MT. Random $\ddot{y}_T$ and y_N signals were obtained from magnetic tape recordings, and the initial heading error was introduced as an initial condition (not shown). The missile aerodynamics were simulated by mechanization of the equations of motion, (7), and the limited maneuverability was represented by appropriate limits imposed on the control position, δ, where it appears in the simulation. The radome diffraction characteristic was simulated by means of a padded-potentiometer function generator. The quantity e in figure 5 represents the relative displacement, $y_T - y_M$, of the target and missile from the reference line of sight. At the end of the attack, e is the miss distance. The remainder of the simulation, that is, the radar, control system gain λ, computer, and autopilot, was set up in the form shown in figures 1 and 2. The final values of the design parameters were determined by trial-and-error testing as discussed in the next section.

Design of the Control System

The trial-and-error procedure.- The principle of rationing the available missile acceleration, described previously, was employed in the trial-and-error design because it is an easier criterion to evaluate than miss distance (the ultimate criterion) when system inputs are random. This is because each simulated attack gives only one value of miss distance whereas the same run yields an entire time history of missile acceleration (or equivalently, of commanded acceleration, a_c). Each such time history can be analyzed to estimate how much of the commanded acceleration, in an rms sense, is useful line-of-sight information and how much is due to disturbances. The design procedure then consists in adjusting system gains and other parameters to achieve a reasonable balance between the two effects. Miss distance performance of the system so designed can then be ascertained by a number of additional runs.

The radar.- The exact form of the radar transfer function was found to have little bearing on the problem, the only important criterion being the speed of response. A simple second-order transfer function of the form

$$Y_R = \frac{1}{(0.04\ s + 1)(0.3\ s + 1)} \tag{8}$$

was employed, where the 0.3-second time constant is the principle factor in controlling the speed of response.

The gain, λ.- The hypothesis that the gain should be reduced as the flight progresses was verified in the simulation study by trying various types of constant and time-varying gains. The gain function shown in figure 6 was found to give good performance in terms of providing satisfactory correction of launch errors, following line-of-sight inputs, and avoiding the build-up of noise-induced errors. The initial value of the gain, λ_o, is such as to give an over-all system gain (from $\dot{\sigma}$ input to a_M output) of 53,000 ft/sec^2 per radian/sec, a value which gives rapid correction of the initial heading error with little trajectory overshoot. The gain remains constant at this value for about half the flight and then decreases linearly to a final value at intercept of 5300 ft/sec^2 per radian/sec. It is of interest to note that the so-called navigation ratio of the system (the expression commonly employed for the gain of proportional navigation systems), given by the relation λ/V_M, has an initial value of 11.3. This is a much higher value than is normally employed in homing systems, but the simulation study indicated that there is no difficulty in using so high a gain at long ranges as long as the gain is reduced at shorter ranges.

The autopilot.- The final autopilot design is shown in block diagram form in figure 7. The configuration is typical of acceleration-type autopilots. Simplifying assumptions which have been made are that the control-position servo and the instruments which supply the feedback terms are ideally fast (i.e., have unity transfer functions). The servo output, δ, is limited to represent the real limits on control position, and the output of the integrator is also limited to prevent integrator "wind-up" at times when the controls are against their stops.

A word of explanation is necessary regarding the K_{B1} and K_{B2} feedback paths. It is noted that if the integrator were linear K_{B1} and K_{B2} could be combined as a single feedback of $\dot{\theta}$ introduced after the integrator. However, with this arrangement a marked increase in damping would result whenever the integrator output saturates. Since a slightly underdamped response is desired under all conditions (to insure rapid closure of the sample-and-hold gate following a $\dot{\theta}$ transient), measures should be taken to avoid damping increase. Splitting the feedback in the manner shown serves this function.

Values of the forward loop gain, K_a, and the feedback gains, K_A, K_{B_1}, and K_{B_2}, found to be satisfactory are given in figure 7. With these constants and the given aerodynamics the over-all transfer function of the autopilot-aerodynamics combination in the linear region is:

$$\frac{a_c}{a_M} = \frac{0.99\ (-0.0096\ s^2 - 0.00022\ s + 1)}{(0.27\ s + 1)(0.059\ s^2 + 0.23\ s + 1)} \tag{9}$$

It is seen that the system is third order, the quadratic term having a natural frequency of 0.66 cps and damping of 0.47, and the first order term having a time constant of 0.27 second. The zeros at approximately $s = \pm 10.2$ have little effect on the response.

Step responses of the autopilot for small and for large (saturating) a_c inputs are shown in figures 7(b) and (c). The initial negative portion of the a_M transient is caused by the zeros of the transfer function. It will be noted that the response is not unusually fast. Of particular interest is the length of time from the beginning of the transient until the first $\dot{\theta}$ zero crossing, which is seen to be about 1 second. This period has a primary influence upon the average length of time the sample-and-hold gate remains open.

The computer.- Values of the gate level, A, and the gains, K_H, K_{C_1}, and K_{C_2}, found to be satisfactory are given in the block diagram representation of the computer shown in figure 2. It will be noted that the value chosen for K_H gives a time constant of 0.1 second for the sample-and-hold circuit. This time constant is a compromise choice, being large enough to give some filtering action against noise but still small enough to permit rapid pickup whenever the gate closes. The values selected for K_{C_1} and K_{C_2} give an open-loop pseudo transfer function for the compensation loop of the form:

$$G_C = \frac{500\ \dot{\theta}_R^2\ (0.1\ s + 1)\ \lambda/\lambda_o}{s(0.04\ s + 1)(0.3\ s + 1)} \tag{10}$$

The compensation loop is nonlinear because the gain varies as $\dot{\theta}_R^2$, but closed-loop stability can be judged from a root locus plot for G_C, which indicates that the closed-loop poles are sufficiently well damped for all expected values of $\dot{\theta}_R^2$. With the maximum value of λ, the "natural frequency" of the compensation loop lies in the range from 0.6 to 3.8 cps for $|\dot{\theta}_R|$ in the range 0.1 to 0.4 radian/sec, thus insuring adequate response without too great a sensitivity to noise. As λ becomes smaller, this natural frequency range decreases.

PERFORMANCE EVALUATION

Description of the Tests

To provide a basis for judging the degree of success achieved by the modified system in reducing the effects of radome diffraction, miss-distance measurements were made (using an analog simulation) for a conventional sluggish control system, for the system modified to decouple radome feedback, and for a so-called perfectly compensated system. Four different test conditions were investigated in each case to ascertain the relative influence of the random target maneuver and the noise upon the miss distance. These conditions were: (1) no $\ddot{y}_T$ or y_N (initial heading error only); (2) no $\ddot{y}_T$ but with y_N; (3) no y_N but with $\ddot{y}_T$; (4) with both $\ddot{y}_T$ and y_N. Since the inputs were random processes (except for the initial heading error), a number of simulated flights for each condition were necessary to obtain a reasonable statistical measure of miss-distance performance.

The Sluggish System

The conventional system tested was one in which the autopilot was made sluggish enough to insure system stability in the presence of the given radome diffraction feedback characteristic (fig. 4). An analog simulation was employed to design this autopilot, the choice of system parameters being made to give as good a step response as possible under the restriction that the over-all control system, including the k feedback, be reasonably stable. Although this system cannot very well be said to be optimum, still it seems about as simple an engineering choice as could be made under the circumstances and is representative of systems actually in use.

The sluggish autopilot configuration is shown in figure 8(a) and its step response is illustrated in figures 8(b) and (c). It is noted that the configuration is simpler than that of the fast autopilot designed for the modified system. Because the system is so sluggish (i.e., K_a small), the response is not importantly affected by K_A and K_{B1} feedbacks as employed in the fast autopilot, and these are not used. A constant control system gain, λ, of 53,000 was used in contrast to the time-varying λ of the modified system because the low-pass characteristic of the autopilot so completely removes the effects of noise that there is no justification for the inclusion of a time-varying λ. In fact, a time-varying λ may actually hurt the performance of the sluggish system by rendering it even more sluggish than necessary at short ranges.

Results of the sluggish system tests are given in tables I and II and figure 9 for cases with and without target maneuvers, showing average miss distances of 674 and 380 feet, respectively. Noise was not introduced in these tests because the system was quite indifferent to it and it served merely to render the a_c time histories more difficult to analyze. Typical trajectories and corresponding time history plots of a_c, a_m, and $\dot{\theta}$ are shown in figure 10.

The Modified System

Results of the miss-distance measurements made with the modified system are given in tables I and II, and the distribution of miss distance for the target maneuver cases is shown in figure 9. It is seen that with the random target maneuver, an average miss distance of about 130 feet is experienced, and that the effect of noise is trivial. Trajectories and time histories for typical runs with and without target maneuver are shown in figure 11.

The Perfectly Compensated System

To obtain a measure of the influence of radome diffraction on the miss-distance performance of the modified system due to imperfect compensation, miss-distance measurements were made for a so-called perfectly compensated system. Such a system is artificial but nevertheless serves as a convenient reference for performance comparisons. The perfectly compensated system was simulated by simply omitting the radome diffraction and computer from the modified system while retaining the same radar, time-varying gain, and autopilot.

Results of the tests of this system are given in tables I and II and figure 9. The indication is that the random target maneuver produces an average miss distance of about 93 feet and that the influence of noise is trivial. Typical trajectories and the corresponding time histories of a_c, a_M, and $\dot{\theta}$ are given in figure 12 for test conditions (2) and (4).

Discussion of the Results

The most important observation to be made is the significant performance advantage which the modified control system possesses relative to the sluggish autopilot system by virtue of the decoupling of the radome diffraction feedback. A 10 to 1 advantage in miss distance is seen in the case when there is no target maneuver and a 5 to 1 advantage with the assumed random maneuver. The reason the improvement is greater with no

target maneuver is that much of the miss distance experienced by the sluggish system is due to inability of the system to cope satisfactorily with the initial heading error, which the modified system does very well.

Comparison of the miss-distance figures for the perfectly compensated and modified systems indicates that the trial-and-error approach has been successful in achieving a reasonably efficient system design, in that the modified system experiences only a 40 percent greater average miss distance than does the perfectly compensated system. The difference is attributable to the effects of residual (uncompensated) radome diffraction in the modified system. It should be noted, however, that the comparison made here provides a somewhat optimistic appraisal of the success of the modified system. This is because the perfectly compensated system as defined here is restricted by being forced to utilize the same radar, time-varying gain, and autopilot as the modified system. In theory, if perfect compensation were possible, a control system with better performance could be designed, and the true measure of the residual effect of radome diffraction should be based on a comparison with this superior system.

Success of the design in a different sense, that is, in terms of efficient use of the available acceleration, is indicated from an examination of the typical no-target maneuver time history shown in figure 11(a). It is seen that an appreciable amount of unnecessary maneuvering occurs, largely because of the residual radome diffraction, compounded somewhat by the effects of the noise. However, after the initial heading error is corrected, the rms level of a_M is less than 1 g, which is well within the maneuvering limits of the missile. Thus, there is adequate following of target maneuvers when they occur.

The fact that there is no significant difference between the noise and no-noise average miss distances requires some comment. The reason for this behavior is that the system has had to be made relatively insensitive to noise to enable the compensation scheme to operate with reasonable efficiency. In the process, the system has inevitably been rendered somewhat poorer in following target maneuvers and in discriminating against radome diffraction perturbations than would have been possible if the noise were not present. Thus, even though the effects of noise do not appear explicitly in the miss-distance measurements, the indirect effects due to the restrictions imposed on the system design are undoubtedly appreciable.

A word should be said about the distribution of miss distances shown in figure 9. It is apparent in examining figure 9 that there are too few runs in each of the cases illustrated to provide any more than a rough idea of the miss-distance statistics. For one thing, no significance can be attached to the observed differences between the noise and no-noise conditions. However, the skewing of the distributions in the direction

of negative values of miss is pronounced enough to be significant. This skewing is readily explained by consideration of the unequal plus or minus maneuverability limits which exist in the problem; that is, since the missile can develop more negative than positive acceleration, it is more apt to miss by passing below the target than above when the target executes the random ±1 g maneuver. This effect is compounded by the fact that the missile is initially below the target and must climb to intercept.

ADDITIONAL CONSIDERATIONS

The Two-Channel Control System

When the missile configuration is symmetrical as assumed in this study, it is apparent that both channels of the control system present identical problems. Thus, the yaw control channel can be afforded the same treatment given here for the pitch channel. An added complication arises, however, in considering the complete three-dimensional problem because of radome diffraction cross coupling between channels. For instance, when the missile yaws, there can be an apparent line-of-sight rotation induced by radome diffraction in the pitch channel as well as in the yaw channel. Fortunately, the cross-coupling diffraction parameters should not be as troublesome as the in-channel parameters because the gains associated with the cross-coupled loops are much lower. Nevertheless, some difficulty may be experienced from this source in the realization of an actual system, and additional complexity may be required to cope with it. For instance, it may be necessary to have each gate controlled by both pitching and yawing velocity. If the missile is roll-controlled, no trouble should arise from roll-induced radome diffraction feedback.

Operation at Lower Altitudes

The analysis presented has been concerned with missile operation at high altitudes. At lower altitudes the radome diffraction problem becomes less serious as the control surface effectiveness increases and smaller angles of attack are required for the missile to maneuver. It, therefore, is of interest to consider how the modified system would perform under these conditions. A simple approach to this problem is to recognize that the gain of the radome diffraction feedback loop decreases as the altitude decreases, so that the effect is similar to that obtained when the diffraction itself is assumed to decrease. Additional simulation tests indicated that the modified system operates quite satisfactorily with no radome diffraction, so it appears that no special problem exists. Of course, the autopilot characteristics change markedly as a function of altitude, so that some provision must be made to modify the autopilot as a

function of altitude. Alternatively, an adaptive autopilot might be employed. However, these considerations are beyond the scope of this report.

CONCLUSIONS

A technique has been demonstrated for mitigating the deleterious effects of radome diffraction in a homing missile by the addition of a simple special-purpose computer to a conventional control system. The basic principle involved is making use of information already available in the control system but not normally utilized for this purpose.

It is important to note that the new method does not eliminate the need for a good radome since the method cannot produce perfect results, and system performance is still dependent upon the radome diffraction characteristics. Nevertheless, the technique works well with presently available radomes and obviates the need for possibly unattainable or very expensive improvement in radome quality.

The increased complexity required by the system modification described is of course undesirable. However, this complexity does not appear to be any greater, and may well be less, than that required by any other equally effective approach to the problem. The question the designer must answer is whether the benefits to be gained in improved missile performance outweigh the disadvantage of building a somewhat more complex system.

Various possibilities of extension of the technique to other applications may occur to the reader. In general, any control problem which involves an unwanted and unavoidable feedback phenomenon may be amenable to a similar treatment.

Ames Research Center
National Aeronautics and Space Administration
Moffett Field, Calif., July 6, 1960

APPENDIX

THE RADOME DIFFRACTION PHENOMENON

The radome enclosing the antenna of a homing missile radar tracking system is generally of a conical or ogival shape (for aerodynamic reasons) which inevitably produces distortion of the electromagnetic radiation passing through it to the antenna. Distortion is also produced by uncontrolled dielectric thickness variations which arise in the manufacture of the radome shell, and by the proximity of portions of the missile frame to which the radome is attached. In addition, thermal and mechanical stresses are apt to develop in the radome during flight to produce generally unpredictable further distortion of the radiation pattern as seen by the radar.

To the radar system this distortion looks like an angular displacement of the missile-to-target line-of-sight, the amount of displacement being a function of the look angle, or angle of incidence of the radiation upon the radome. The geometry of this situation for the vertical plane is illustrated in figure 13, where it is seen that the apparent line-of-sight angle, σ_a, is in error by the amount ϵ:

$$\sigma_a = \sigma - \epsilon \tag{A1}$$

Differentiation of equation (A1) yields

$$\dot{\sigma}_a = \dot{\sigma} - \frac{\partial \epsilon}{\partial \beta} \dot{\beta} \tag{A2}$$

where β is the look angle and $\partial\epsilon/\partial\beta$ is the so-called error slope, or change in ϵ as a function of β. From figure 13, it is seen that $\beta = \dot{\sigma} - \dot{\theta}$ and by definition $k = \partial\epsilon/\partial\beta$. Thus equation (A2) becomes

$$\dot{\sigma}_a = \dot{\sigma}(1 - k) + k\dot{\theta} \tag{A3}$$

It should be noted that for good radomes the value of k rarely exceeds 0.1, so that the gain change represented by the factor $(1 - k)$ is relatively unimportant and is ignored in the present study. Equation (A3) can therefore be written

$$\dot{\sigma}_a \approx \dot{\sigma} + k\dot{\theta} \tag{A4}$$

Inasmuch as $\dot{\sigma}$ can be regarded as the input and $\dot{\theta}$ as an output of the control system, expression (A4) indicates that radome diffraction can be regarded as a feedback of pitch rate, $\dot{\theta}$, in the amount k.

The analysis given here is for a two-dimensional case. A three-dimensional study would require that radome diffraction feedback of roll and yaw rates be included.

The electromagnetic radiation distortion which is characterized by the parameter k is assumed in this report not to be known explicitly; that is, the functional relationship between β and k is expected to differ somewhat for each radome installation and, even in an individual case, will probably vary (slowly) with time in a generally unpredictable manner. A scheme for compensating radome diffraction cannot therefore depend on a priori knowledge of the k function. However, it is necessary to consider the general nature of radome characteristics in order to undertake a realistic test program of a proposed compensation technique. A typical k function selected for use in this study is shown in figure 4, where it is noted that k is an even function of β as a result of the symmetry of the radome about its longitudinal axis. Slow changes in k as a function of time need not be considered here because they do not affect the operation of the system developed herein.

REFERENCES

1. Tice, Thomas E. and Fouty, Robert, eds.: Proceedings of the OSU-WADC Radome Symposium, June 1957, Vols. I & II. WADC Technical Report 57-314.

2. Fouty, Robert, and Greene, W. A., eds.: Proceedings of the OSU-WADC Radome Symposium, June 1958, Vols. I & II. WADC Technical Report 58-272.

3. Stewart, Elwood C., and Smith, Gerald L.: The Synthesis of Optimum Homing Missile Guidance Systems With Statistical Inputs. NASA MEMO 2-13-59A, 1959.

TABLE I.- MISS-DISTANCE AVERAGES FOR RUNS WITHOUT TARGET MANEUVER

	Without noise	With noise
Sluggish system	380 ft (1 run)	
Modified system	40 ft (5 runs)	36 ft (7 runs)
Perfectly compensated system	20 ft[a] (1 run)	30 ft (6 runs)

[a]The no-noise, no-target-maneuver case should produce zero miss distance. The nonzero value actually observed is a result of inaccuracies and noise in the simulation and recording equipment employed. The basic accuracy of the measurements is considered to be within ±20 feet.

TABLE II.- MISS-DISTANCE AVERAGES FOR RUNS WITH RANDOM TARGET MANEUVER

	Without noise	With noise
Sluggish system	674 ft (23 runs)	
Modified system	143 ft (30 runs)	118 ft (28 runs)
Perfectly compensated system	98 ft (30 runs)	88 ft (28 runs)

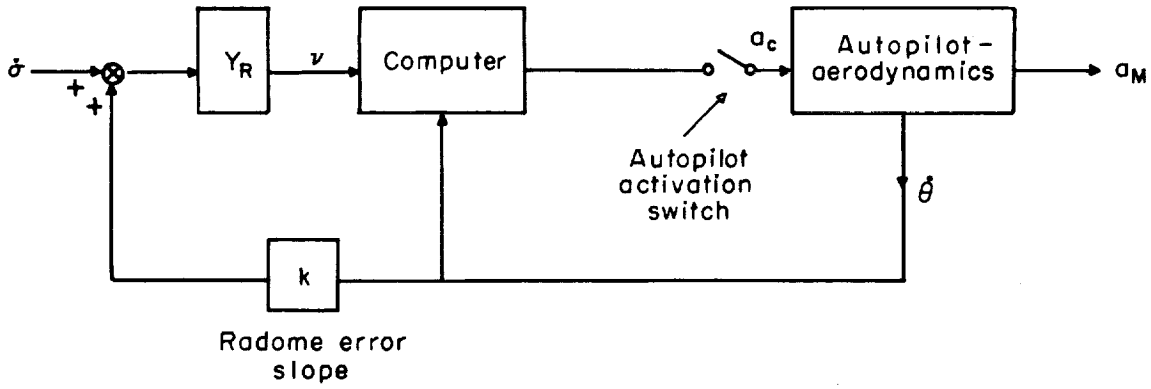

Figure 1.–Control system block diagram.

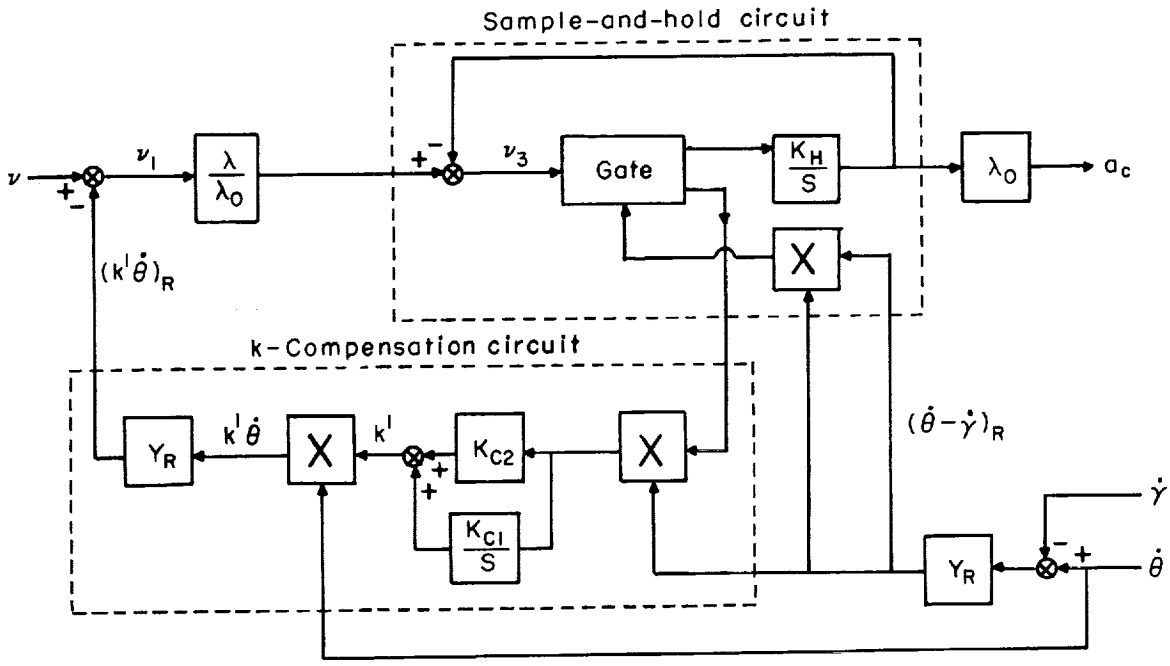

Gate operation: Gate connects ν_3 to $\begin{cases} \text{hold integrator when } (\dot{\theta}-\dot{\gamma})_R^2 < A^2 \\ \text{k-compensation circuit when } (\dot{\theta}-\dot{\gamma})_R^2 > A^2 \end{cases}$

Design parameters:

$A = 2.5 \times 10^{-2}$ (rad/sec)^2

$K_H = 10$

$K_{C1} = 500$

$K_{C2} = 50$

λ/λ_0 = time-varying system gain (see figure 6).

Figure 2.—Computer block diagram.

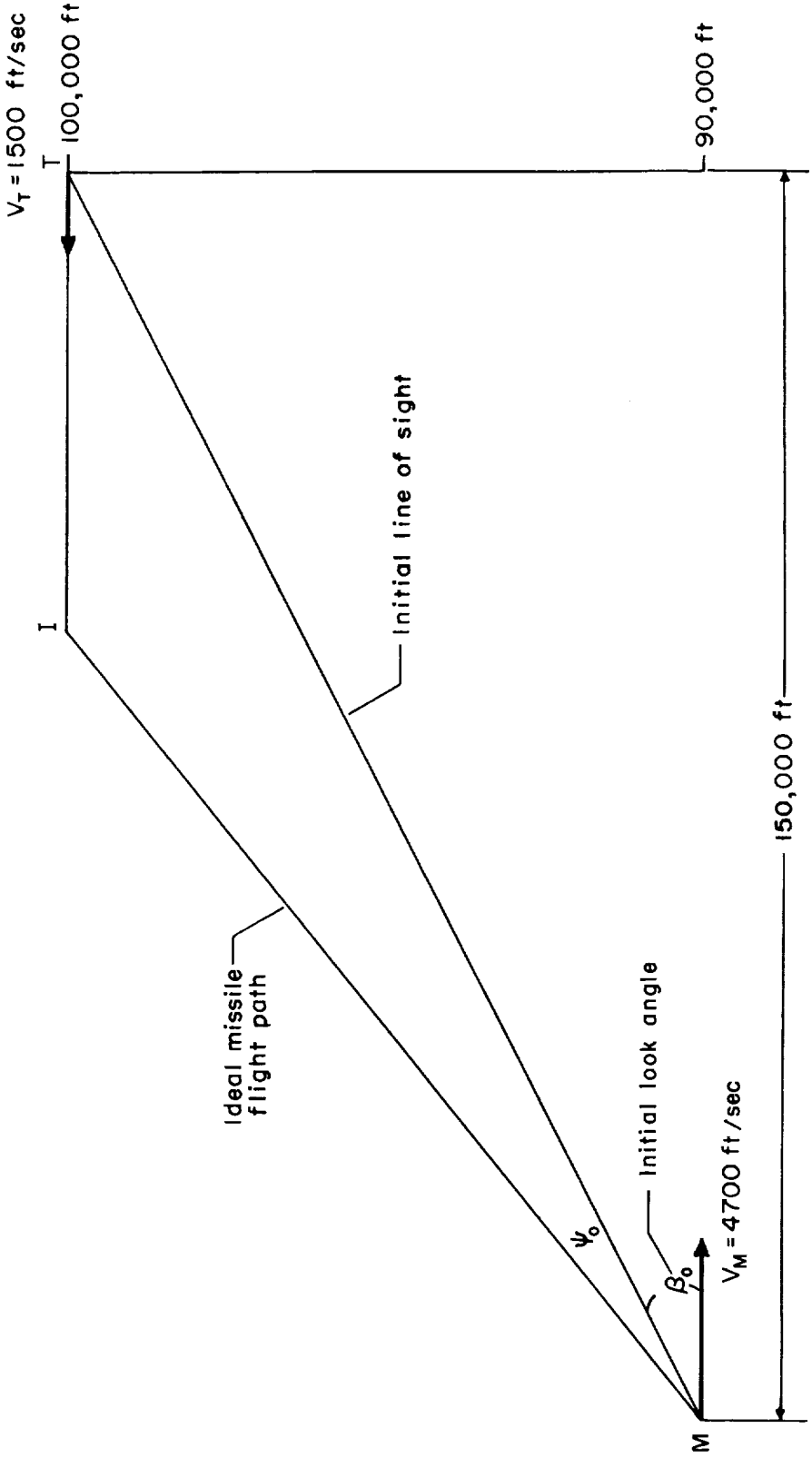

Figure 3.- Geometry of the assumed attack situation.

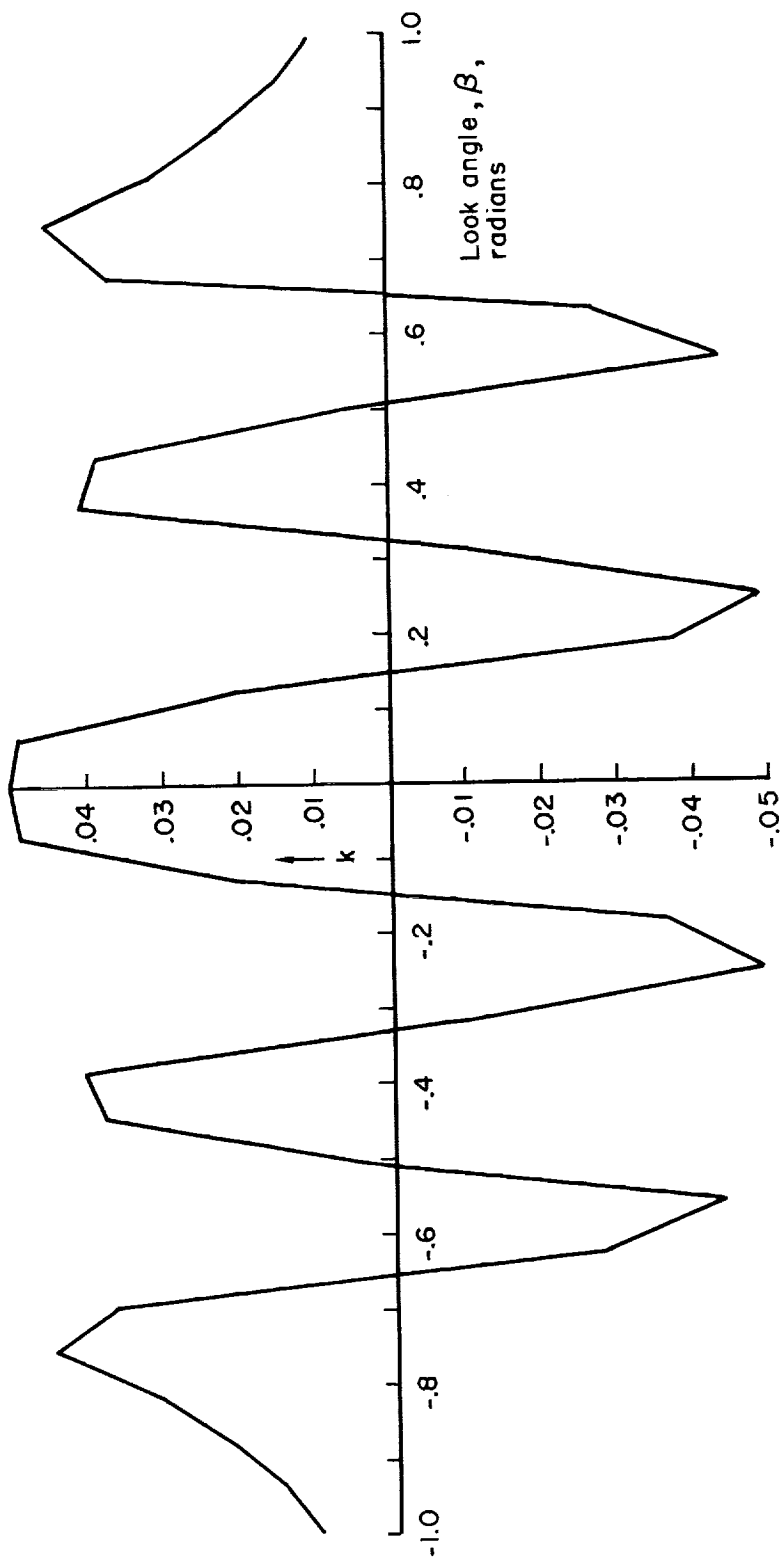

Figure 4.- Assumed radome error slope characteristic.

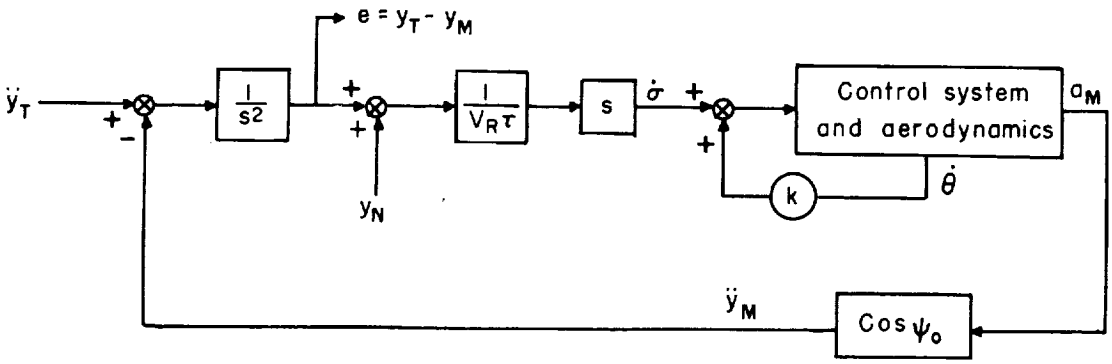

Figure 5.- Block diagram of the homing missile attack simulation.

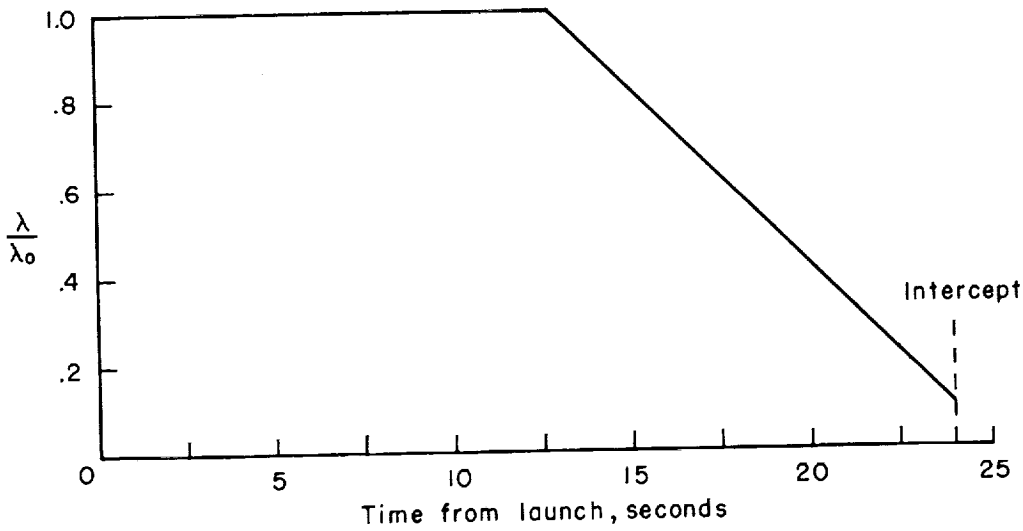

Figure 6.- Time-varying system gain.

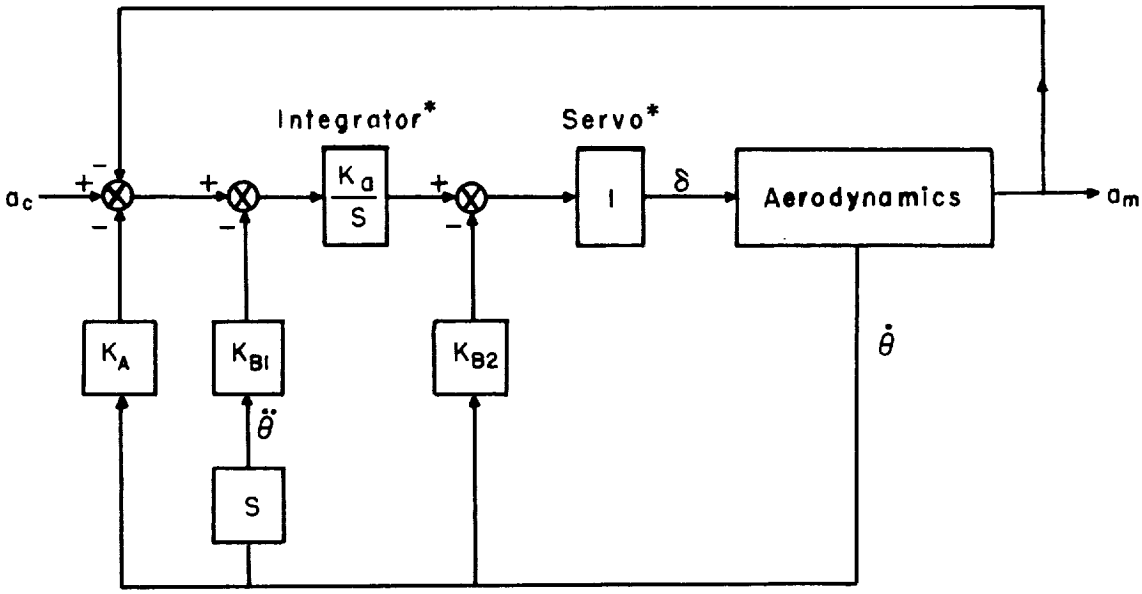

* Integrator and servo outputs limited at ± 0.5 radian

Design parameters:

$K_a = 0.02$
$K_A = 62.5$
$K_{B1} = 16.7$
$K_{B2} = 0.4$

(a) Block diagram.

Figure 7.- Modified system autopilot.

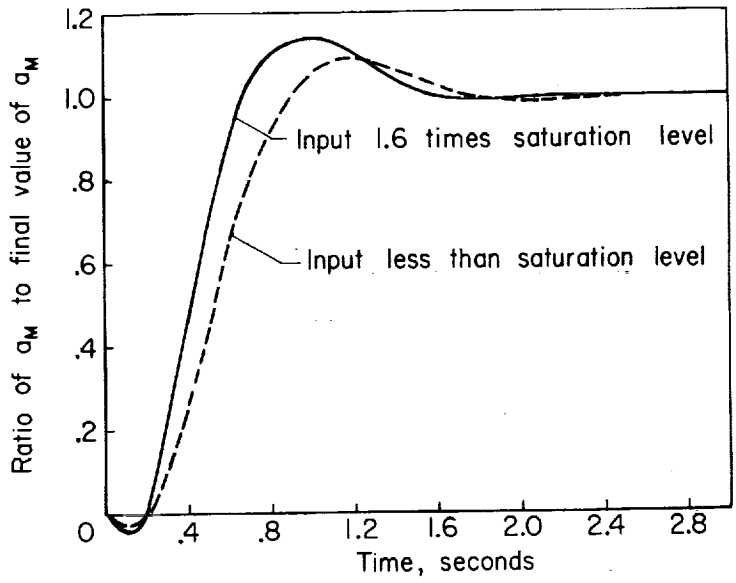

(b) The a_M response to a step command.

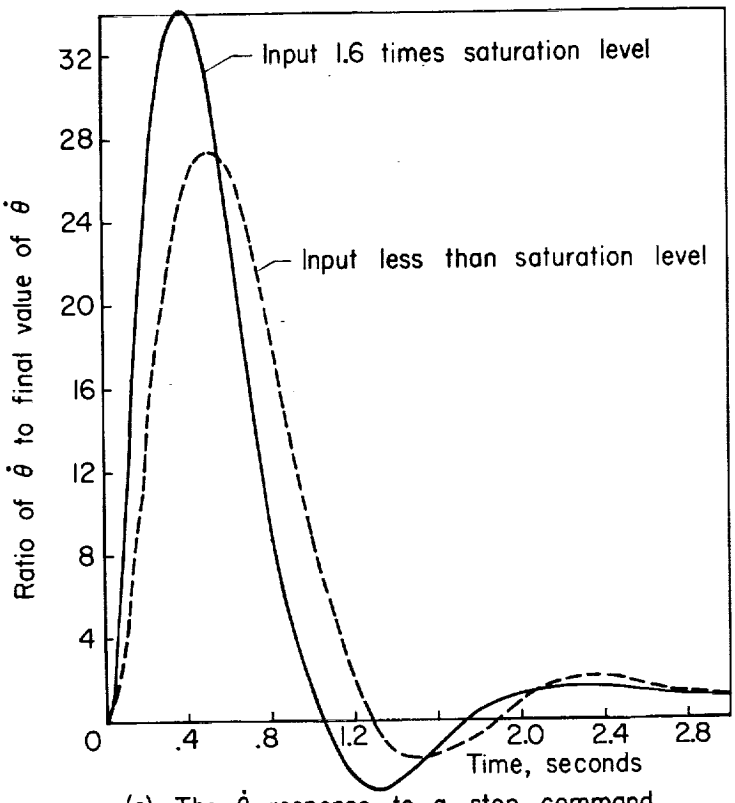

(c) The $\dot{\theta}$ response to a step command.

Figure 7. - Concluded.

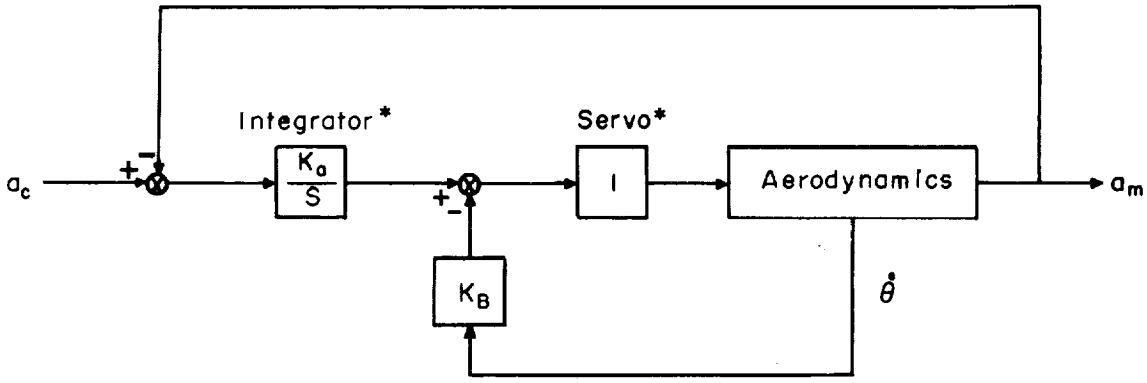

*Integrator and servo outputs limited at ±0.5 radian

Design parameters:

$K_a = 0.0008$

$K_B = 0.4$

(a) Block diagram.

Figure 8.–Sluggish autopilot.

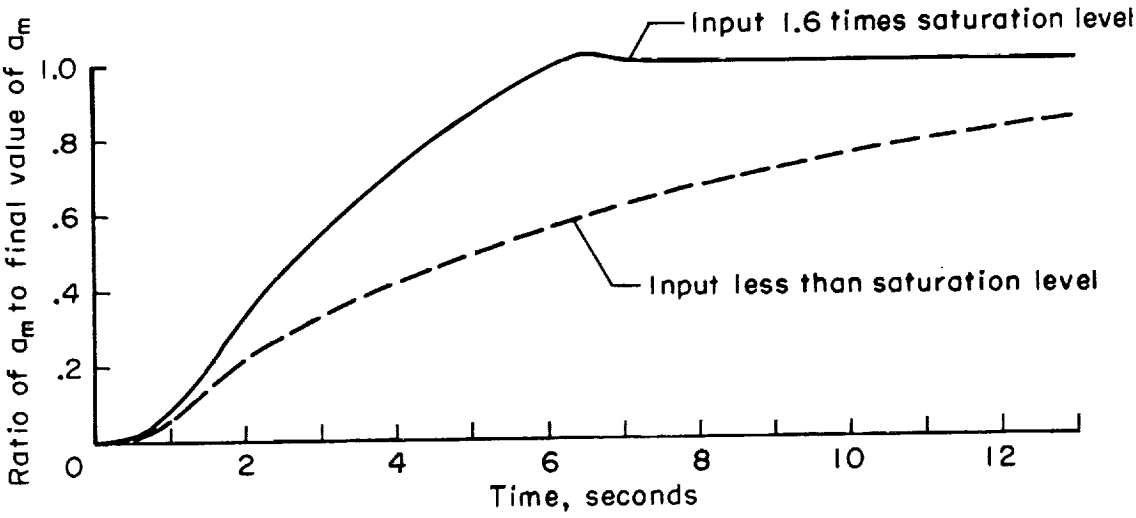

(b) The a_m response to a step command.

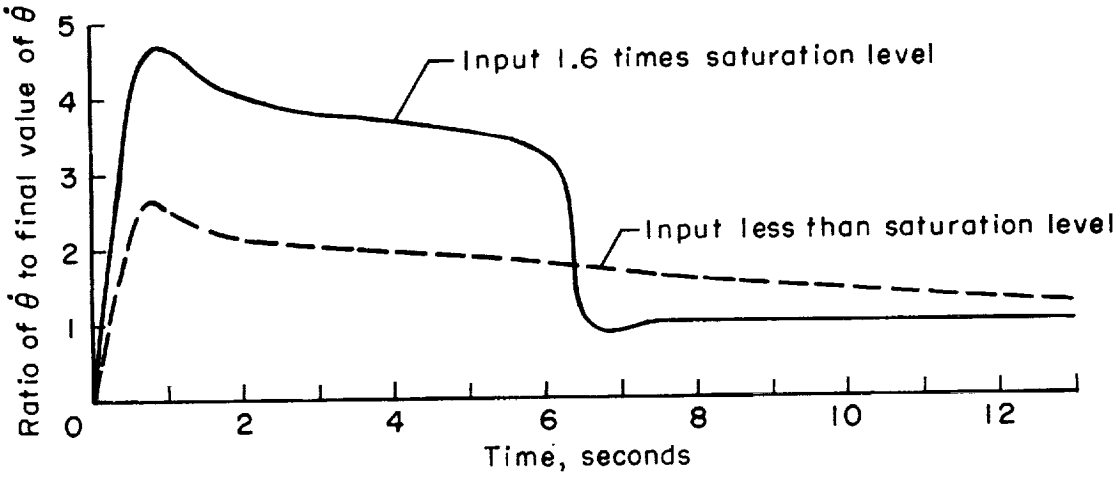

(c) The $\dot{\theta}$ response to a step command.

Figure 8. – Concluded.

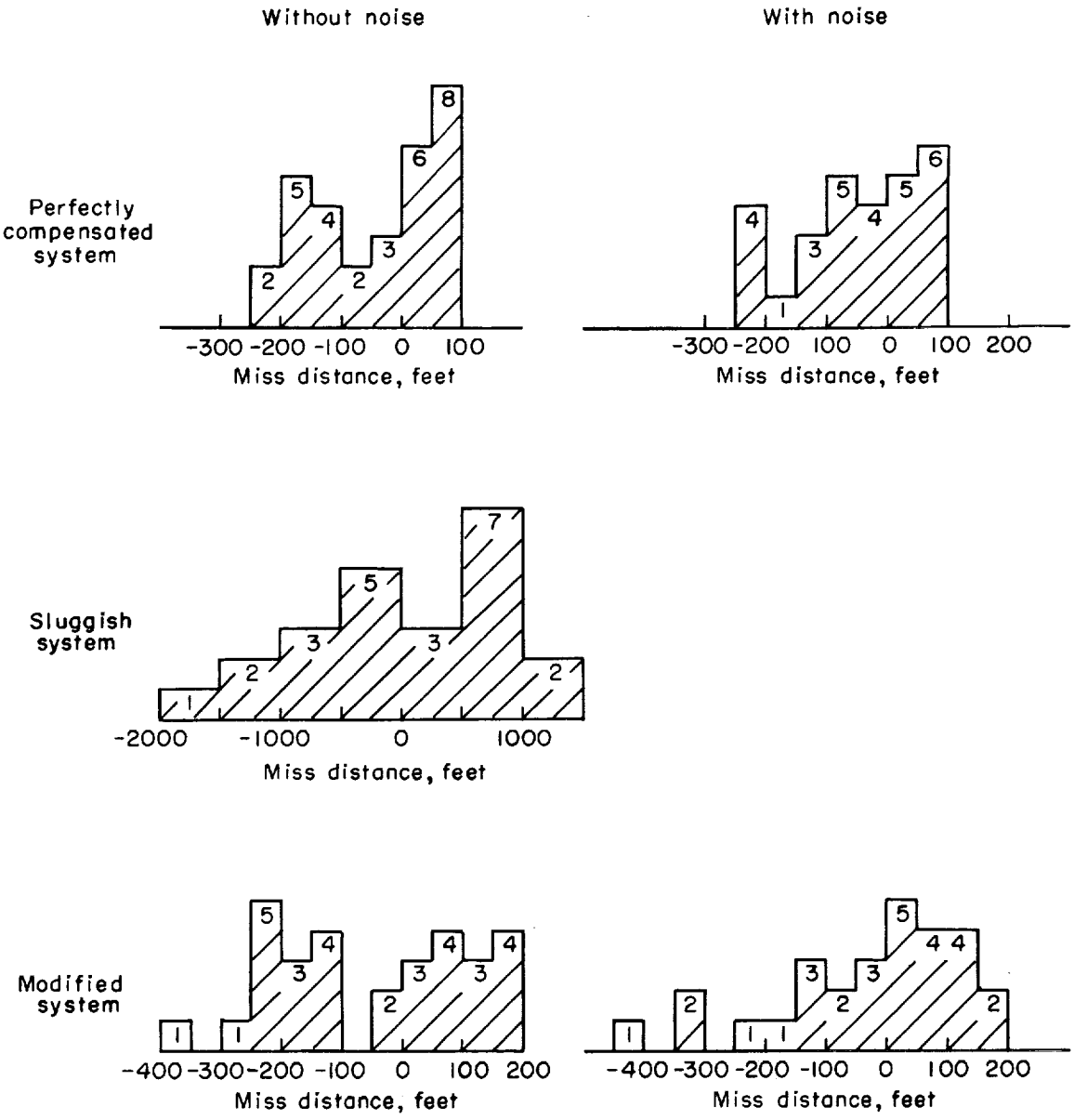

Figure 9.- Distribution of miss distance measurements for target maneuver runs.

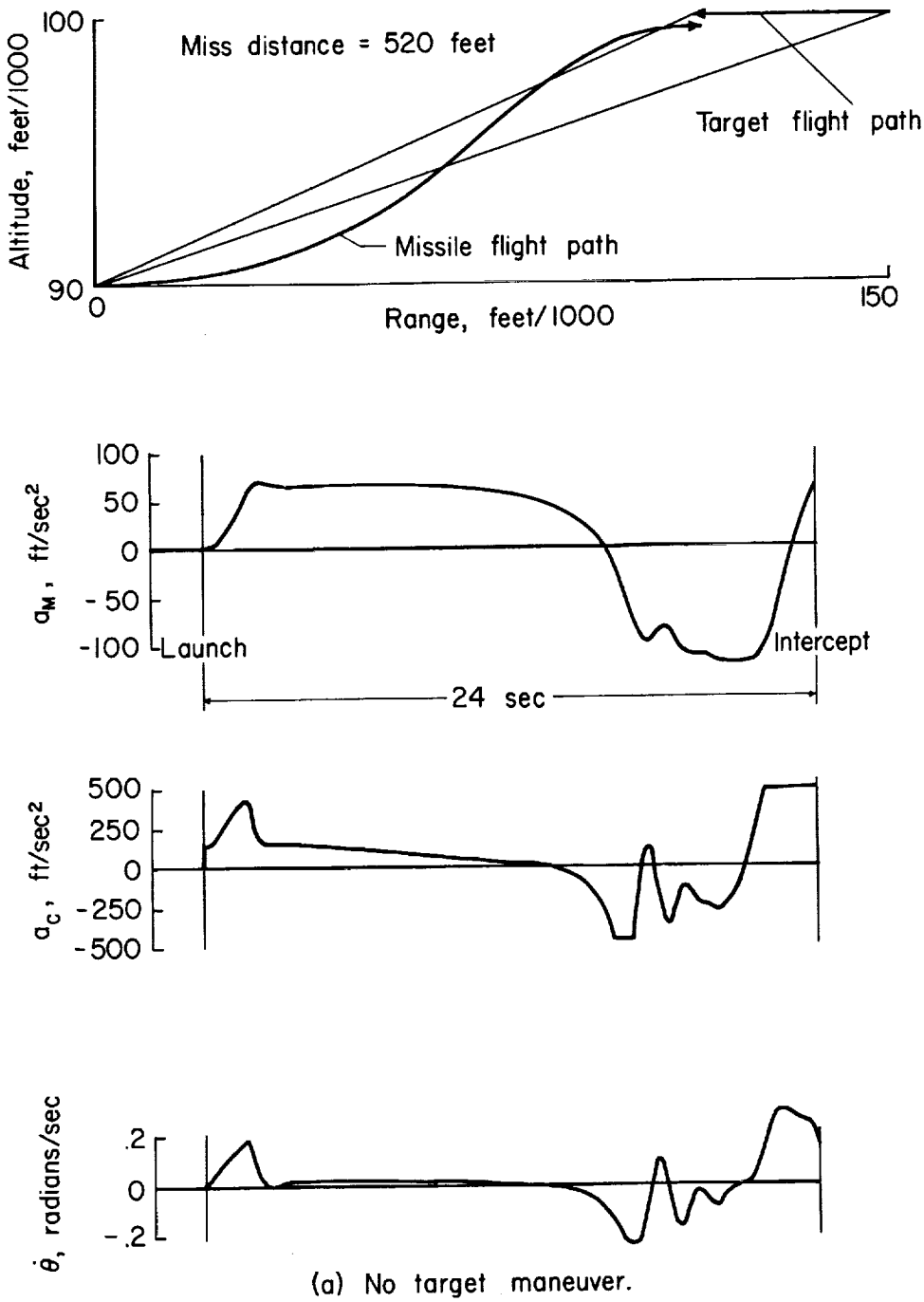

(a) No target maneuver.

Figure 10.- Typical trajectories and time histories with an initial heading error for missile with sluggish autopilot.

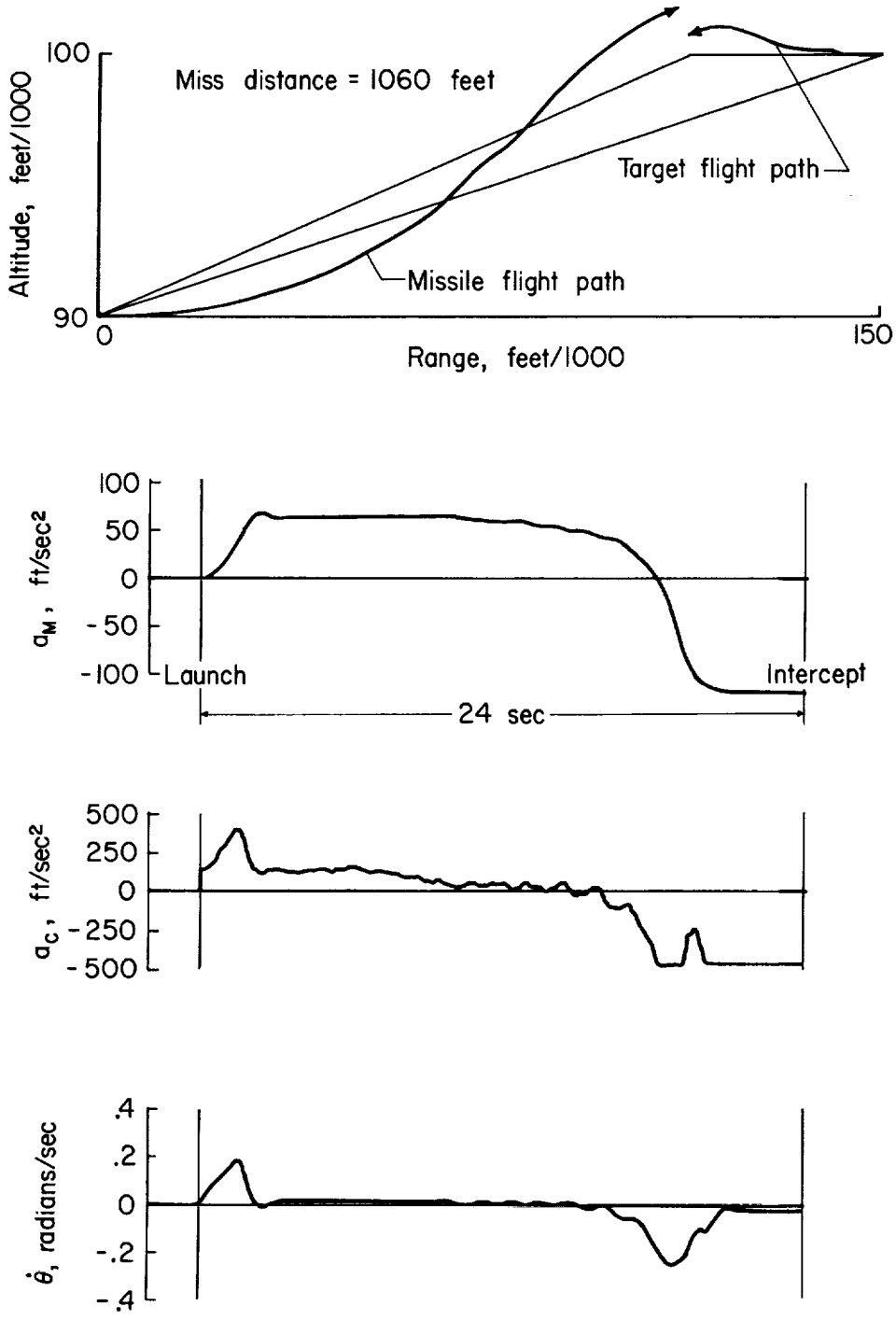

(b) Random target maneuver.

Figure 10. - Concluded.

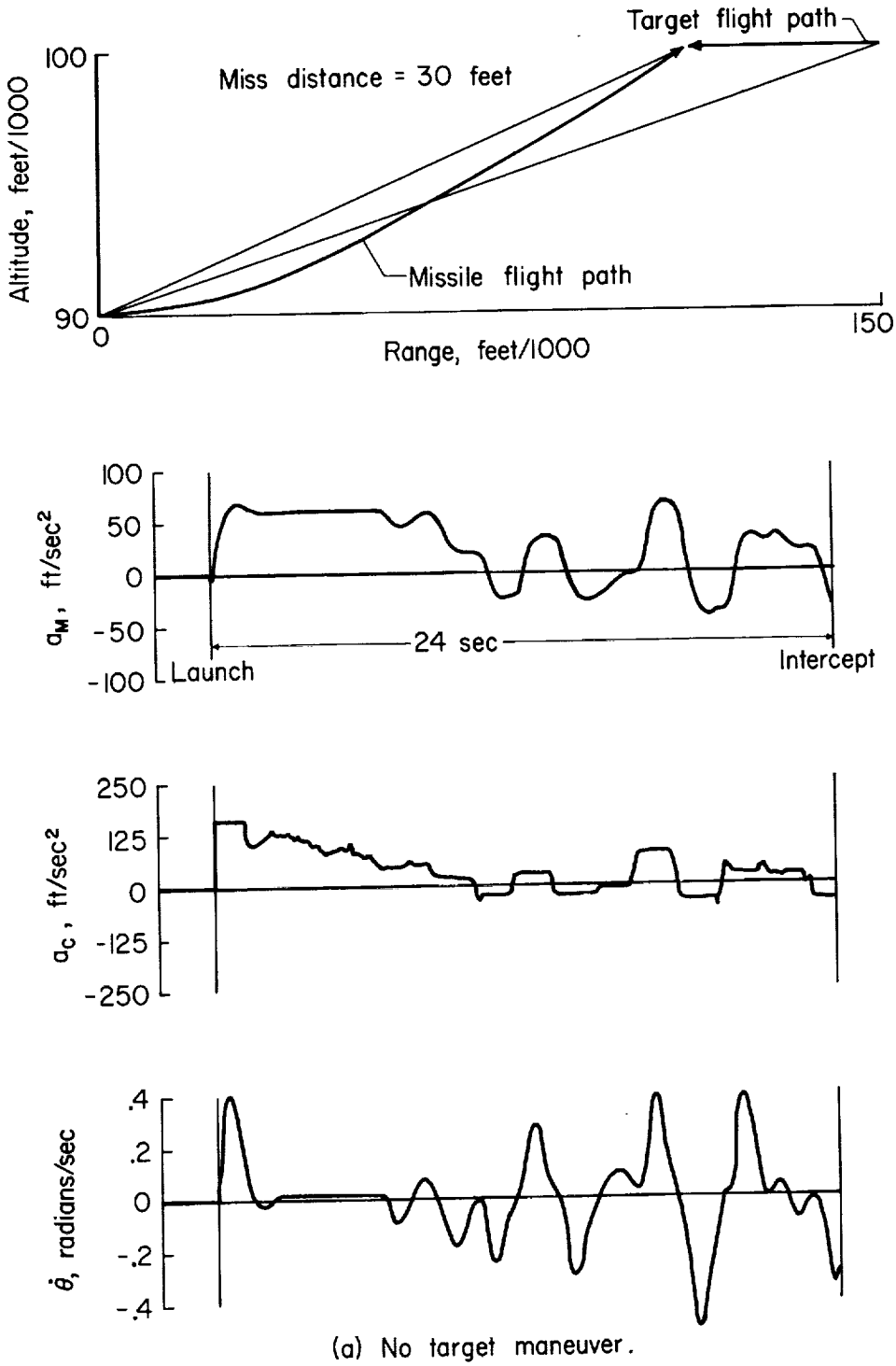

(a) No target maneuver.

Figure 11.- Typical trajectories and time histories with initial heading error and noise for missile with modified control system.

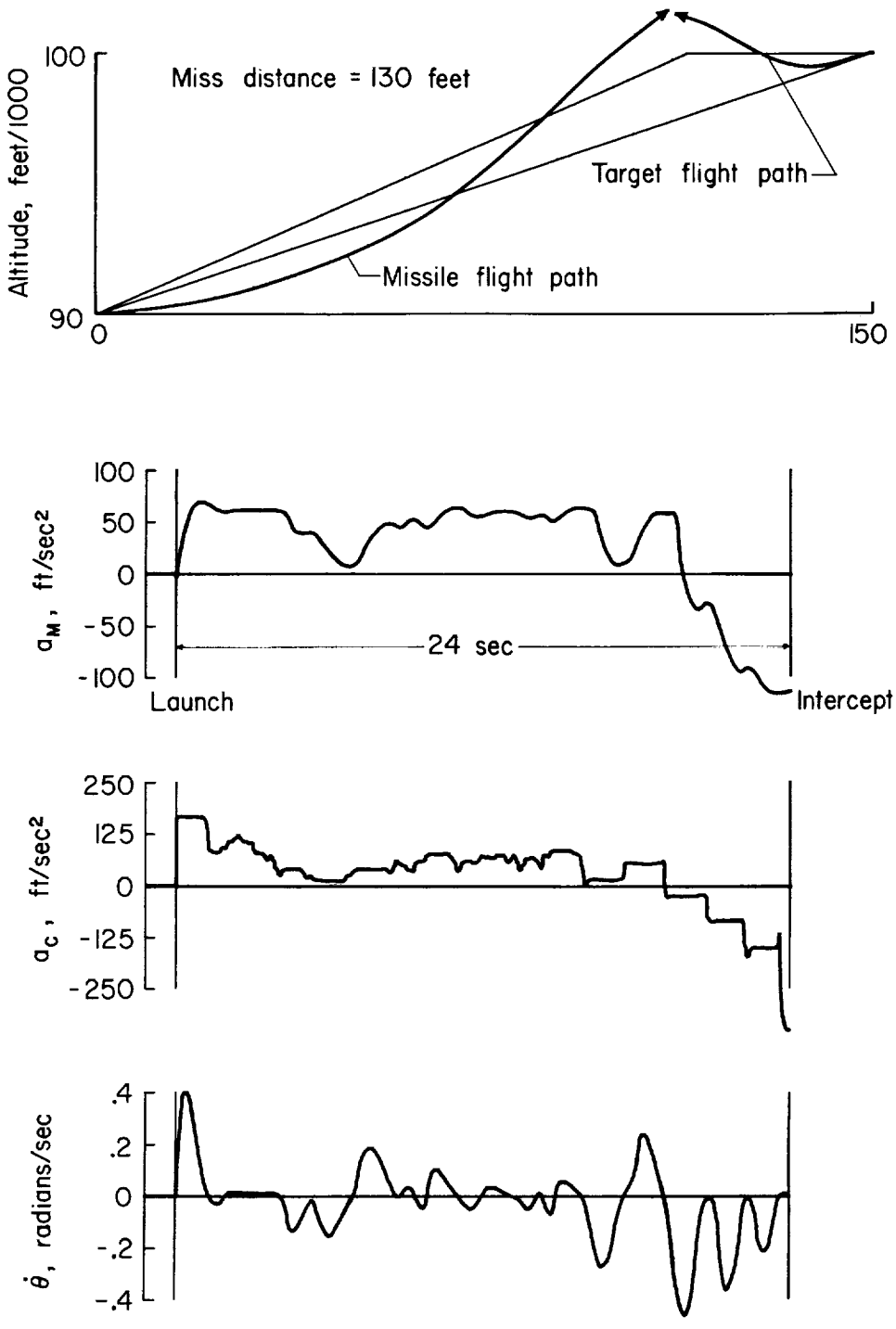

(b) Random target maneuver.

Figure 11.- Concluded.

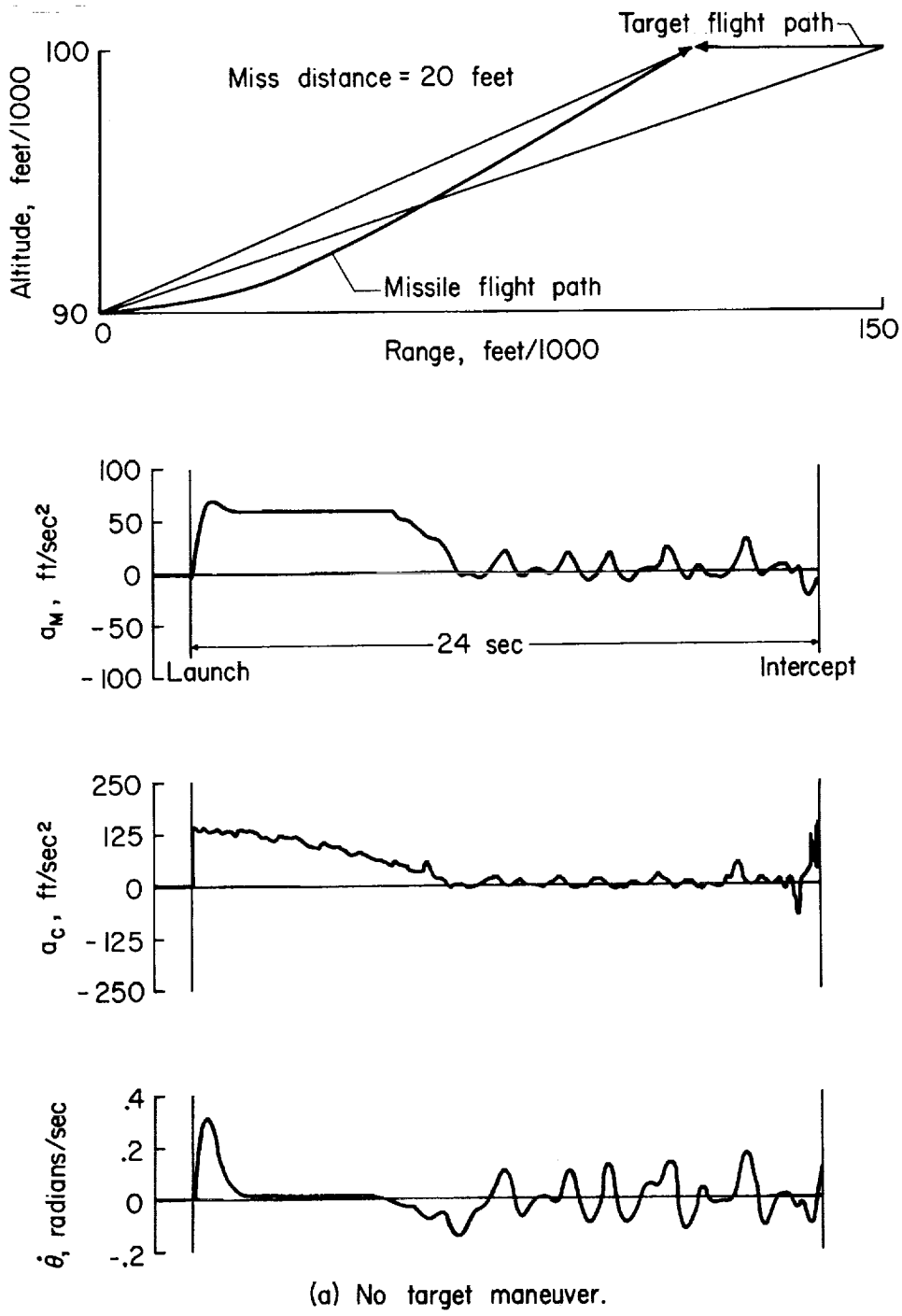

(a) No target maneuver.

Figure 12.- Typical trajectories and time histories with initial heading error and noise for missile with perfectly compensated control system.

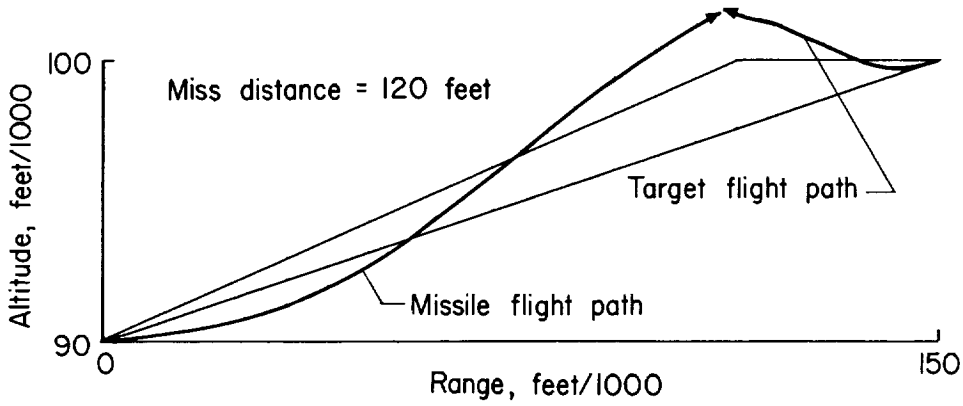

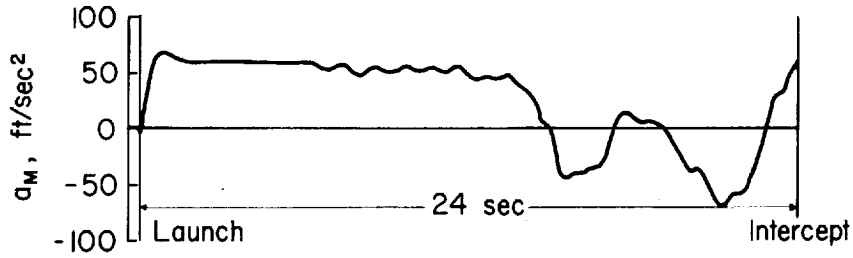

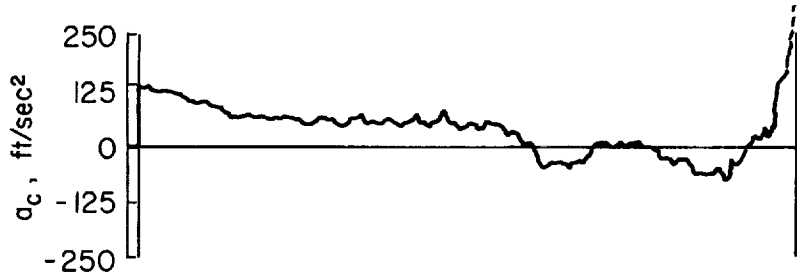

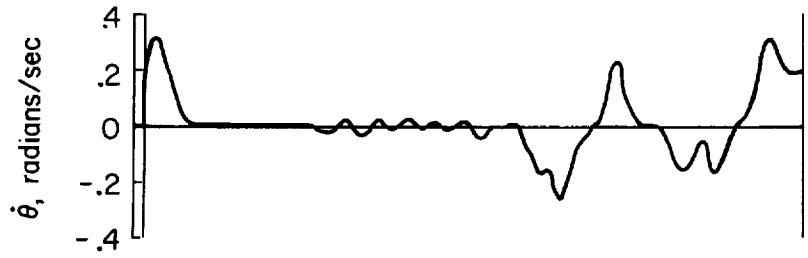

(b) Random target maneuver.

Figure 12.- Concluded.

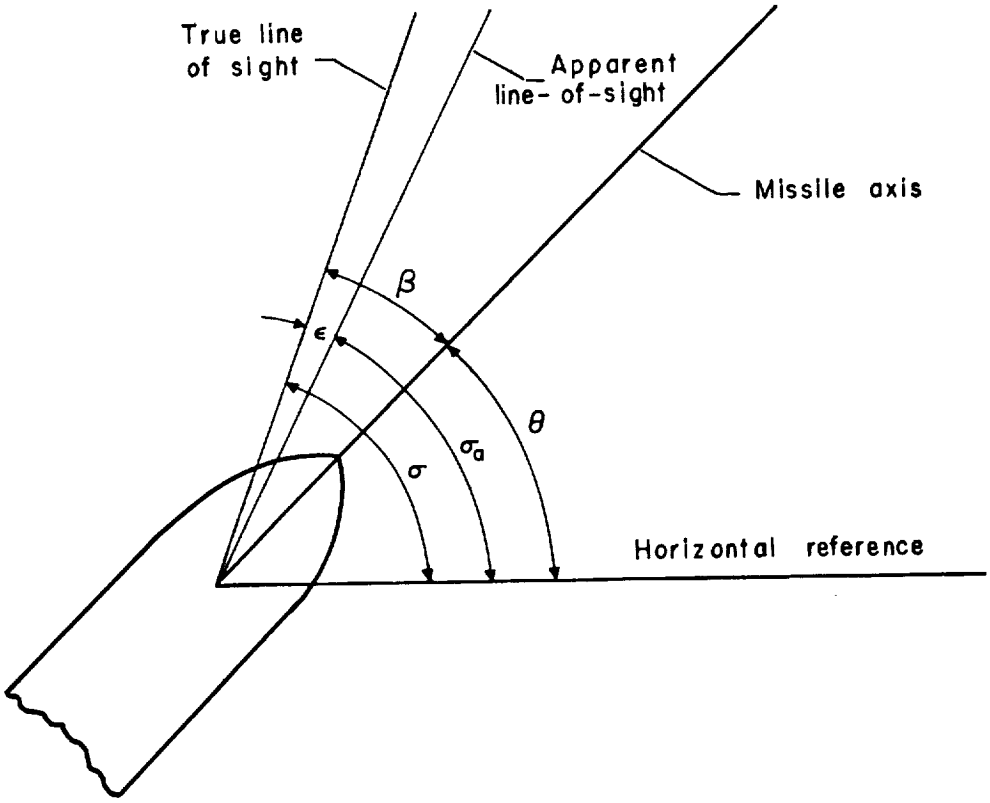

Figure 13.- Geometry of radome diffraction.